UAB

Assessing soil respiration variability in a Mediterranean ecosystem: a baseline for monitoring an underground H$_2$ storage in Seville, Andalucia.

Thesis author

Miguel Sánchez Pérez

Supervisors

Javier de Elio Medina

José Manuel Sánchez Biec

Bernat Claramunt

Workplace

AUTHOR'S CONTRIBUTION

The research for this master's Thesis titled "Assessing soil respiration variability in a Mediterranean ecosystem: a baseline for monitoring an underground H_2 storage in Sevilla, Andalucía." was initiated in May 2024 and completed in January 2025. This thesis has been carried out by Miguel Sánchez Pérez as a scientific study, as part of the master's program in Terrestrial Ecology and Flora and Fauna Management, with a specialization in terrestrial ecology. The student's contribution to each task is detailed as follows:

- Experimental design: Developed by the student in collaboration with the project team (Javier de Elio Medina, Luis Felipe Mazadiego). Student's contribution: 60%.

- Fieldwork: Conducted jointly with the project team, although some campaigns were carried out independently by the student. Student's contribution: 80%.

- Data analysis: Performed 95% by the student, with support from the supervisor.

- Discussion and writing: Drafted by the student with appropriate revisions provided by the supervisor (Javier de Elio Medina). Student's contribution: 95%.

DECLARATION OF ORIGINALITY

I, **Miguel Sánchez Pérez**, holder of **ID 77850423T**, declare that this master's Thesis is original and has been conducted in full compliance with copyright regulations, always ensuring proper citation of all sources.

A B S T R A C T

To reduce fossil fuel dependence and greenhouse gas emissions, underground hydrogen storage (UHS) of green hydrogen produced via electrolysis is emerging as a promising solution for the future. After fossil fuel combustion, soil disruption is the second largest source of CO_2 emissions, as it releases carbon stored in these natural sinks. Arid and semi-arid ecosystems, such as the Mediterranean, covering over two-fifths of the Earth's surface, are highly sensitive to moisture availability, and their response to climate change remains uncertain. As part of the Measurement, Monitoring, and Verification (MMV) program for an experimental UHS project in Sevilla (Andalucia), a baseline assessment of soil respiration (Rs) was conducted, along with a gas chromatography campaign, to detect potential risks early on. Seasonal variability was analyzed through multiple field campaigns, considering temperature, soil moisture, and different land uses, including a pine forest, a riparian zone, and olive orchards under distinct management practices. Results showed that Rs was highest in autumn and lowest in winter. The riparian zone exhibited the highest Rs (18.3 g/m²/day CO_2), while the pine forest (9 g/m²/day CO_2), extensive olive orchards (8.3 g/m²/day CO_2), and intensive orchards (7.4 g/m²/day CO_2) had more similar values. Within olive orchards, distance to the nearest tree, and soil vegetation cover were significant predictors, whereas row/inter-row position was not. However, during summer, higher Rs values were observed in row areas. Ultimately, no evidence of micro-seepage risk was found, but further investigations and additional monitoring campaigns are recommended.

Keywords: Underground hydrogen storage (UHS), micro-seepage, gas baseline, soil respiration (Rs), olive orchard, drought Mediterranean, land uses, land management, seasonal variability, spatial variability, row inter-row, linear-mixed models, temperature correlation.

1.Introduction

Our excessive reliance on consumption of fossil fuels as a primary energy source has caused an alarming rise in atmospheric carbon dioxide levels. This emission rate continues to grow in a world where energy demand and consumption are on the rise due to population growth and higher living standards, as well as industrial and technological evolution in developed countries (Oliveira et al., 2021a; Pablo-Romero et al., 2023). However, this production system is not sustainable anymore and alternative, much cleaner option, should be developed (e.g., "Goal 7: Affordable and Clean Energy" of the United Nations;(UN, 2025)). At European level, the strategy for the energy transition is defined in the REPowerEU plan, with the aims of: i) a 55% reduction in CO_2 emissions by 2030 compared to 1990 emissions; ii) achieving net-zero emissions by 2050; and ii) a proportion of 42.5% renewables in electricity generation (European Commission, 2024)

In the transition to a sustainable energy production, renewable sources will be essential (Zeng et al., 2023). In this sense, solar and wind energy will be the driving forces in the global energy market, and it is expected that they surpass 50% of the electricity supply. However, a renewable energy-based generation, in which energy production will fluctuate with atmospheric conditions (e.g., sunlight level and in tensity, wind force) and geographical constraints which when combined with annually varying energy demand results in renewable energy excesses or deficits. This implies that there must necessarily be an energy storage system to regulate the differences between supply and demand (Heinemann et al., 2021a; Oliveira et al., 2021a; Shiva Kumar & Lim, 2022).

One option to overcome this limitation, and cover longer periods of time, is through the use of green hydrogen (Oliveira et al., 2021b). Hydrogen is one such promising environmentally friendly renewable energy carrier, as it is easily converted into electricity or heat, and it can be used to store and transport huge amount of energy (Hassan et al., 2023; Rosen & Koohi-Fayegh, 2016). Although it is not readily available directly on the earth, it is available in chemically combined forms of water, fossil fuels, and biomass. Hence the main challenge is to separate hydrogen from the naturally occurring compounds efficiently and economically. Solar, wind and tidal energies are prepared and well suitable renewable power sources for green hydrogen production through water electrolysis due to their widespread power distribution. The combination of renewable energy with water electrolysis is particularly more advantageous because it balances the discrepancy between energy demand and production.

However, and although hydrogen boasts the highest energy-to-mass ratio among fuels (excluding nuclear), its low energy density necessitates large storage volumes compared to other energy vectors like natural gas (Hassanpouryouzband et al., 2021). Conventional storage methods like surface tanks and pipelines are constrained by limited storage and discharge capacities, despite their widespread use. Underground Hydrogen Storage (UHS) emerges as a promising solution for meeting large-scale and long-term storage demands capable of accommodating energy capacities in the GWh to TWh range over weeks or months (Ciotta & Tassinari, 2024; Gabrielli et al., 2020; Tarkowski, 2019).

The long experience with the geological storage of other gases like CO2 in Carbon Capture and Storage project (CCS) (Kalam et al., 2021) and CH4 (Al-Shafi et al., 2023),

suggest that the storage of H_2 will be also feasible and safe for the environment. However, it implementation is still in the early stages, with a limited number of projects where H_2 has been injected in salt-cavern and saline aquifer (Ciotta & Tassinari, 2024; Gal et al., 2019). In this regard, for a successful storage operation, a storage play consisting of 1) a porous and permeable reservoir to store the gas, 2) an impermeable caprock to prevent vertical gas leaking, and 3) a trap structure to avoid lateral gas escape (Heinemann et al., 2018). Salt caverns, saline aquifers and depleted gas fields provide a wide range of hydrogen storage scales and deliverability, being the last one the most frequent and popular natural gas storage option (Heinemann et al., 2021b; Miocic et al., 2023).

Some of the challenges faced in underground hydrogen storage are, site selection, geochemical reactions, microbial growth in reservoir, well integrity, geological integrity of caprock, and leakages and seepages. Leakage refers to subsurface migration away from the primary containment due to breaches like faults or compromised wells, while seepage involves hydrogen escaping to the atmosphere or surface waters (Elío, 2024). Seepage can be manifested as macro-seepage (large, detectable flows) or micro-seepage (smaller, dispersed flows that are harder to detect). Hydrogen macro-seepages are unlikely with proper site selection and management. However, micro-seepages are more probable due to hydrogen's physicochemical properties (Elío, 2024; Thiyagarajan et al., 2022). As pure hydrogen is non-toxic, non-poisonous, non-corrosive, and environmentally benign, the environmental risks associated with leakage or seepage are limited compared to leakage of $CH4$ or $CO2$, but it could have a cascade of environmental, social and economic risks.

Ensuring the success of underground hydrogen storage (UHS) requires a robust Measurement, Monitoring, and Verification (MMV) program to detect potential issues early and ensure operational safety (Elío, 2024). Monitoring techniques are categorized into deep methods, which evaluate reservoir integrity and fluid movement, and surface methods, which detect emissions such as gases or brines. Geochemical surveys (e.g., soil gas, surface gas fluxes, surface water) are examples of these near surface techniques. In this project, I am focused on the second ones (Heinemann et al., 2021b).

Surface monitoring is a critical tool for identifying anomalous gas concentrations and tracing the origins of subsurface emissions. Establishing baseline gas fluxes from soil to the atmosphere is essential to differentiate between natural and storage-related emissions which allows for the detection of deviations that may indicate micro-seepages (Elío et al., 2013; Förster et al., 2006; Gal et al., 2019). Additionally, soil gas concentration at the subsurface (e.g., 1 meter deep) provides detailed gas characterization that may help to distinguishing natural gases from those migrating from geological layers or storage reservoirs (Laier & Øbro, 2009).

In underground hydrogen storage (UHS), surface monitoring focuses on detecting primarily hydrogen emissions. However, H_2 is easily consumed by microorganisms and, thus, H_2 concentration can be low at the subsurface even under the presence of micro-seepage (Elío et al. 2024) and the measurement of its degradation by-products (i.e., CH_4, CO_2) would be also useful in a MMV program . Furthermore, these gases may also be injected with hydrogen in the reservoir as cushion gases, stabilizing reservoirs and enhancing storage efficiency (Ma et al., 2019; Panfilov et al., 2006) and thus they are also prone to leak from the reservoir and produce seepage. Besides, they are also produced naturally due to soil respiration and microbial metabolic processes and their baseline

should be established. Baseline estimation aims to predict the storage system's future evolution and support numerical modeling. These studies should start before operations begin and span different seasons to capture variability (Elío et al., 2011).

Soil respiration, what is also is known as soil-CO_2 evolution, efflux or flow, therefore, refers to the release of CO_2 from soil into the atmosphere. This process is governed by the rate of CO_2 production in the soil, the concentration gradient between the soil and atmosphere, and numerous climatic, meteorological, biotic, physical and land-related factors, which affect the movement of CO_2 through the soil (Lardo et al., 2015a). Five main biogenic sources of CO2 efflux from soils have been distinguished, they are root respiration, rhizomicrobial respiration, decomposition of plant residues, the priming effect induced by root exudation or by addition of plant residues, and basal respiration by microbial decomposition of soil organic matter (SOM) (Rayment & Jarvis, 2000)(Kuzyakov, 2006). When we measure the CO2 emitted by the soil, we are capturing all these indicators and understanding how environmental variables influence all these factors is essential.

The rate of CO_2 production is a key indicator of organic matter decomposition and the amount of carbon lost from the soil, accounting for over 25% of global emissions (Maestre & Cortina, 2003; Schlesinger & Andrews, 2000). Net ecosystem uptake is often the residual between two large axes, similar in magnitude but opposite in sign (i.e. photosynthetic carbon uptake and respiratory carbon loss), and consequently a relatively small increase in the rate of soil respiration may be sufficient to switch an ecosystem from carbon sink to carbon source (Martínez H et al., 2008; Raich & Schlesinger, 1992; Rayment & Jarvis, 2000). Given the magnitude of these fluxes and the large pool of potentially mineralizable soil carbon, any increase in soil CO_2 emissions in response to environmental changes could further elevate atmospheric CO_2 levels, reinforcing positive feedback to global warming. (Raich & Tufekciogul, 2000)

Arid and semi-arid ecosystems, covering over two-fifths of the Earth's surface, play a key role in global carbon cycling, as soil respiration (Rs) is highly sensitive to moisture availability (Maestre & Cortina, 2003). In these regions, irregular precipitation, high evaporation rates, and prolonged droughts contribute to strong seasonal Rs variability (Aranda-Barranco et al., 2024). Mediterranean ecosystems are particularly vulnerable to these climatic fluctuations, and while reduced rainfall is expected to lower Rs, its response to water availability remains complex and not fully understood. Understanding the variability of Rs in Mediterranean ecosystems in response to seasonal changes and land use, as orchard management, is key to predicting system behavior under ongoing climate change. This understanding will support the development of effective strategies to preserve the role of soils as carbon sinks.

Olive cultivation dominates Mediterranean agroecosystems, accounting for over 90% of global production (FAO, 2022), with significant economic, social, and environmental implications for the region. In Andalusia, which contributes 29% of the world's olive oil production (Junta de Andalucia, 2023), traditional low-density plantations rely on periodic tillage for weed control, a practice that accelerates soil erosion, runoff, structure degradation, organic matter mineralization, and soil fertility depletion (Álvarez et al., 2007). As an alternative, herbicides have been widely used for weed management in tree rows or across entire orchards due to their effectiveness and

low cost. However, growing concerns over their environmental impact have led to increasing pressure to reduce their use in olive agroecosystems (Turrini et al., 2017). Recently, irrigation has been introduced to mitigate drought effects, and currently, around 38% of Andalusia's olive groves have adopted irrigation to mitigate drought effects, further influencing Rs dynamics (Montanaro et al., 2023). Sustainable management is key to balancing productivity with the preservation of soil carbon sinks.

Mediterranean agriculture is highly diverse, leading to different Rs responses depending on crop type and management. Intensive cultivation accelerates soil organic matter (SOM) loss, often depleting 30–50% of initial levels. Conventional practices, such as frequent tillage, enhance CO_2 emissions by disrupting soil aggregates and exposing stabilized organic matter to decomposition (Schlesinger & Andrews, 2000). In contrast, extensive and sustainable agriculture favors carbon sequestration, as SOM improves soil structure, moisture retention, and air movement, with lower Rs values expected (Martínez H et al., 2008) Additionally, land use history, pruning, and plant phenology play a crucial role, along with interactions within the vegetative community and microfauna (Lardo et al., 2015a; Martin-Gorriz et al., 2020),

Water availability is considered a key determinant, driving both above- and below-ground processes and creating moisture-dependent seasonal patterns in soil CO_2 emissions. The ability of Mediterranean ecosystems to sustain biological activity under limited water conditions underscores the critical role of soil water storage (Aranda-Barranco et al., 2024; Epron et al., 1999; Tan et al., 2021). Water stress strongly influences root respiration, which accounts for 30–50% of soil CO_2 emissions, particularly in summer when it significantly limits Rs. This effect is closely linked to stomatal closure (Aranda-Barranco et al., 2024; Lardo et al., 2015a). Additionally, considering rain pulse responses is essential for accurate net annual carbon flux estimates in Mediterranean ecosystems (Salinas Alcantara, 2018).

Temperature also plays a pivotal role, with rising temperatures accelerating microbial activity and organic carbon mineralization. However, limited moisture availability can hinder decomposition processes, suggesting a potential correlation between these two variables. Optimal soil moisture occurs near field capacity, where macropores facilitate O_2 diffusion and micropores retain water, ensuring substrate availability for microbial and root activity (Almagro et al., 2009; Epron et al., 1999; Fang & Moncrieff, 2001; Salinas Alcantara, 2018).

Rs variability is not only temporal but also spatial, influenced by multiple factors that can affect its distribution, even in seemingly homogeneous systems like bare-soil olive groves (e.g., soil type, use and management, soil organic carbon (SOC), labile organic matter, vegetative coverture, under canopy or alley, crop's age, etc.) (Aranda-Barranco et al., 2024; Raich & Schlesinger, 1992). Soil respiration (Rs) is positively correlated with soil organic carbon (SOC) content, which is generally low in Mediterranean ecosystems, leading to lower Rs values. However, croplands often exhibit higher Rs than natural ecosystems due to management practices as fertilization, soil aeration, and irrigation that influence carbon and water availability (Aranda-Barranco et al., 2024; Wang et al., 2023).

Proximity to vegetation significantly influences soil respiration (Rs), as areas near trees or denser vegetation release more CO_2 due to increased root activity, organic matter decomposition, and higher biological respiration (Jongen et al., 2011). While some research has explored Rs distribution in mediterranean orchards (Almagro et al., 2009; Aranda-Barranco et al., 2024; Bertolla et al., 2014; Chamizo et al., 2017; Lardo et al., 2015b; Montanaro et al., 2023), the differences between Rs under tree canopies and in alleys remain largely unexamined. Higher Rs is expected near olive trees due to autotrophic root respiration and increased heterotrophic activity from decomposing root-derived substrates. In contrast, Rs in alleys is likely lower, as autotrophic respiration is minimal and organic inputs are scarce (Aranda-Barranco et al., 2024).

This emphasizes the multifactorial nature of soil respiration, highlighting the interplay between water availability, temperature, soil properties, management practices, climate and vegetation dynamics. These findings provide evidence of the complexity underlying CO_2 emissions from soils in semi-arid Mediterranean contexts. The questions we aim to address in this article are, therefore, as follows:

- Establish a baseline for gases (H_2, CO_2, He, Ra) in the footprint of the depleted gas reservoir. Are there potential micro-seepages?

- To what extent do seasonal variability and different land uses affect the biological respiration in a Mediterranean ecosystem?

- How does the biological respiration vary in agricultural fields depending on crop intensity, distance to the nearest tree, and whether the measurement was taken in the row or between rows?

2.Methodology

2.1 Study area

Palancares natural gas reservoir has been selected to conduct the first pilot UHS project in Spain. It is situated in the Aljarafe region, approximately 20 km southwest of Sevilla (Spain) and about 3 km northeast of the nearest urban area (Aznalcázar). The Aljarafe plain is a gently sloping platform with an average slope of less than 3%. The Miocene Guadalquivir-Gulf of Cádiz Basin, explored intensively for hydrocarbons since the 1950s, hosts natural gas reservoirs within the "Arenas del Guadalquivir" formation. These reservoirs consist of turbiditic sandstones deposited 6 to 7 million years ago, confined southwestward beneath an 800-meter-thick average impermeable marl layer (Blue Marls) that acts as a seal preventing gas migration.

Table 1: Palancares reservoir extraction volume and rates.

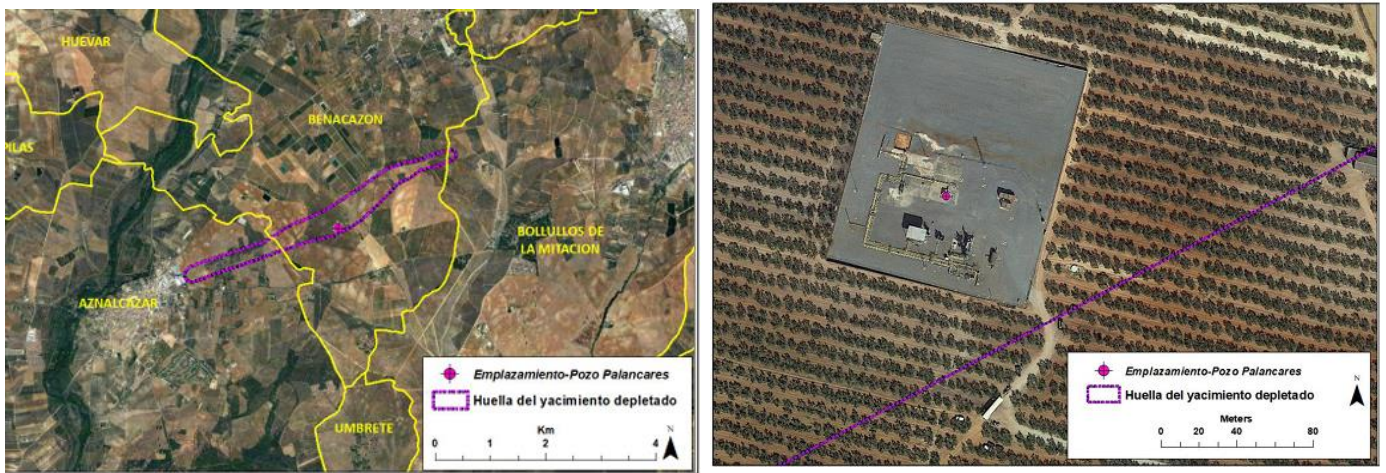| PALANCARES as Underground Natural Gas Storage					
Total Initial Production, Mm3	Remaining gas Injected, Mm3	Void Space in the Reservoir, Mm3/ton H2	Minimum[*] Operating Volume, Mm3 /ton H2	Max. Extraction Rate, m3/d	Max. Injection Rate, m3/d
128.1	10.1	118 / 11.000	65.1 / 6.000	500,000	600,000

Figure 1: a) Palancares location details, and b) zoom around the injection well and infrastructure in Palancares.

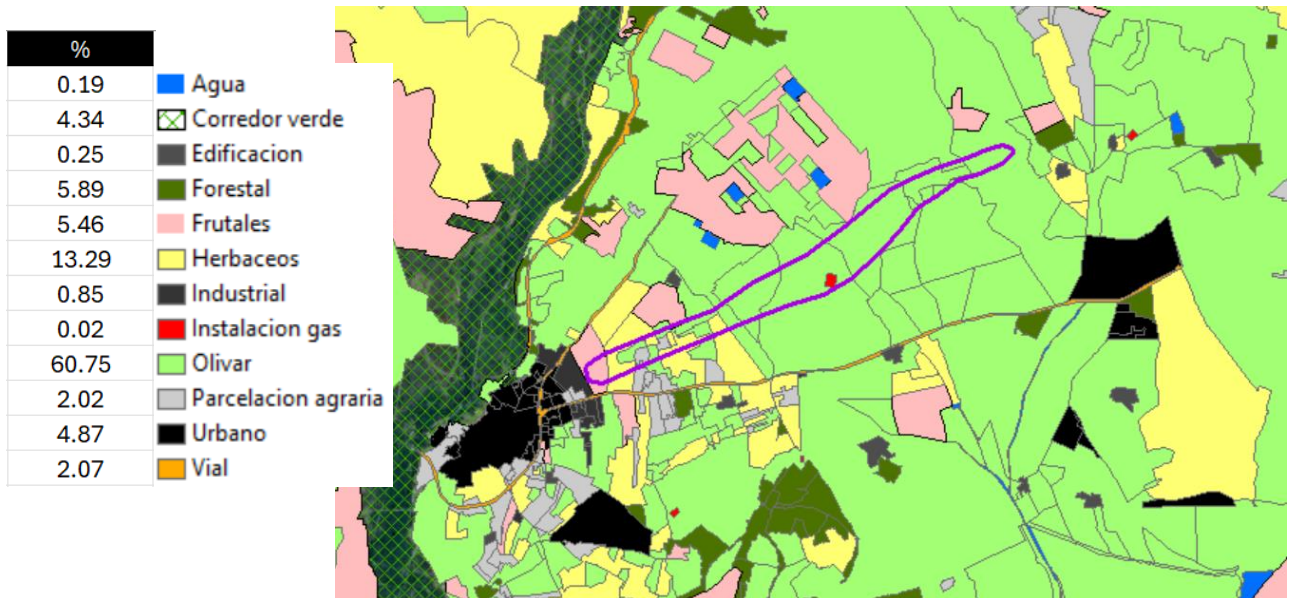| %	
0.19	Agua
4.34	Corredor verde
0.25	Edificacion
5.89	Forestal
5.46	Frutales
13.29	Herbaceos
0.85	Industrial
0.02	Instalacion gas
60.75	Olivar
2.02	Parcelacion agraria
4.87	Urbano
2.07	Vial

Figure 2: Land uses in Palancares surroundings. 1:40000

The footprint of the Palancares reservoir (confined to about 1000 meters depth) is elongated, with a length of about 6 km and an average width of about 300 m. The reservoir is depleted and has been used sporadically since 2013.The footprint includes a platform where gas facilities are located, including the extraction well and gas drying devices. The area is dominated by red soils (luvisols, fluvisols, planosols, cambisols, regosols) with favorable agronomic capacity due to their good water properties (drainage, permeability, and moisture retention) and loamy or silty loam texture, which facilitates root penetration and makes them easy to cultivate.

Most of the footprint consists of private estates with agricultural purposes, almost entirely made up of olive plantations. Additionally, there are also some fruit orchards and grasslands. Based on this information, the area has been divided in three main strata for our analysis:

Guadiamar Green Corridor: The riparian ecosystem develops along the floodplain of the Guadiamar River, characterized by fluvisols and abundant vegetation, including forest formations introduced during the recovery plan after the Aznalcóllar mine disaster (Madejón et al., 2003). This landscape features rich riparian vegetation, annual grasslands, and flora that grows wild and naturally due to minimal human intervention in the management of the riparian forest. The result is a diverse and heterogeneous landscape that contrasts sharply with the predominant agricultural areas along its margins and in the Aljarafe agricultural region.

Palancares Footprint: Crop fields. Mostly olive plantations. The predominant olive variety found is *Olea europaea* var. *Manzanilla* (DIEGO et al., 2017), which exhibits a low, sparse canopy and produces olives primarily intended for consumption as table olives. There are up to 15 estates with different land uses and treatments: plant spacing, use of fertilizers or pesticides, soil aeration with plowing, weed clearing (chemical or mechanical treatments), and irrigation system (irrigated or rainfed). A larger sample size will be collected in this stratum to represent the Rs baseline for MMV program and to recollect the maximum variability of soil treatments concerning CO_2 emissions in crop fields.

The traditional olive grove has disappeared, and the area is now dominated by orchards with different management practices: extensive olive groves (spacing of 10x6 m, 170 trees/ha, 60%-40% soil-to-canopy ratio), semi-intensive groves (7x5 m, 300 trees/ha, 55%-45% soil-to-canopy ratio) and, to a lesser extent, super-intensive hedgerow plantations (5x1.5 m, 1,500 trees/ha, 55%-45% soil-to-canopy ratio) are also present. Within this stratum, measurements were taken in an intensive olive grove planted in 2018, an extensive olive grove and a semi-extensive olive orchard both planted before 1981 and a semi-extensive almond orchard planted in 2020. All measured fields were equipped with an irrigation system, fertilized regularly, and subjected to pruning. Weed management was carried out through superficial tillage using a disc harrow (10–12 cm deep) to remove weeds, aerate the soil, and enhance water infiltration while reducing runoff. However, in the extensive olive grove, herbaceous vegetation was left to grow freely in the alleys, maintaining a more natural ground cover. The fruit was harvested in September, traditionally by hand to minimize damage to the olives. In intensive systems, on the other

hand, mechanical harvesters and tractors were used to optimize efficiency. (DIEGO et al., 2017)

Aznalcazar Pine Forest: pine forest, subject to specific regulations for pine forest areas, that is partially naturalized and exhibits low anthropogenic impact. The coniferous formations are primarily composed of stone pine, accompanied by Mediterranean scrubland species such as cistus, rosemary, and heather, as well as a variety of peri maritime vegetation. These elements collectively contribute to the high landscape value of the forested area. The landscape is relatively homogeneous.
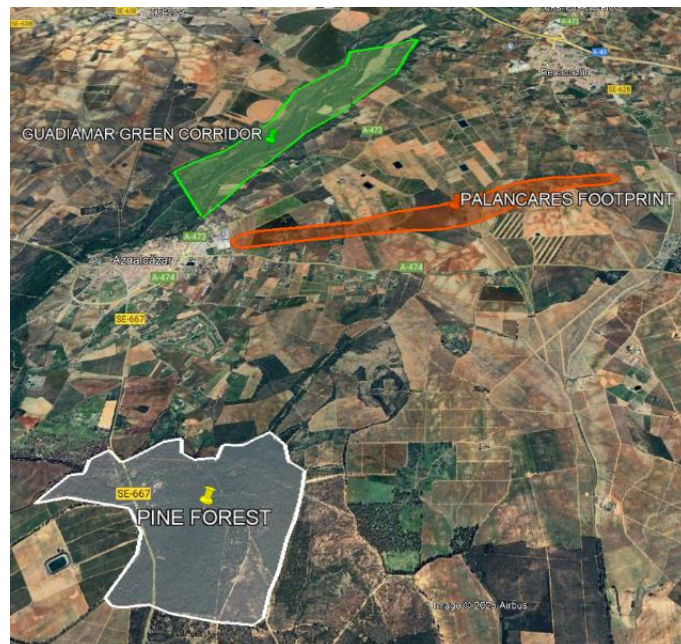

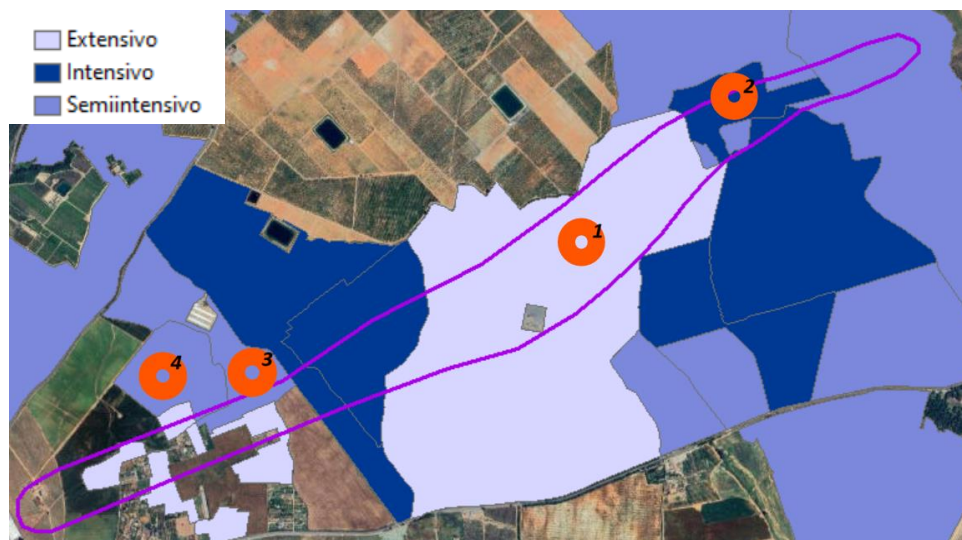*Figure 3: Different strata location around Aznalcázar village.*

Figure 4: Olive groves intensity around Palancares reservoir. The fields where measurements were taken are numbered [1-4] respectively, 1.Extensive Palancares well grove, 2.Intensive grove, 3.Semi-intensive grove, 4.Semi-intensive almond grove.

Figure 5: Sampling Strata: Pine forest (top left), Intensive olive grove in Palancares (top middle), Guadiamar green corridor (top right), Semi-extensive almond grove (bottom left), extensive olive grove (bottom middle), and semi-extensive olive grove (bottom right).

The climate in the study area (i.e., Aljarafe) is classified as hot dry-summer Mediterranean, (Csa) according to the Köppen-Geiger classification. (*Clima Mairena del Aljarafe: Temperatura, Climograma y Tabla climática para Mairena del Aljarafe*, s. f.). It is characterized by warm and dry summers (Jun. – Aug.); daily mean temperatures around 24 - 28 °C and average precipitation of 1 – 3 mm, and template winters (Dic. – Feb.); daily mean temperatures of 10 – 13 °C and average precipitations of 30 – 48 mm. Typically, most precipitation occur in March and April with monthly average precipitation of 75 mm in 10 precipitation days, and there is a clear minimum of precipitation in the summer period (table 2)

Table 2: Summary table of meteorological parameters in Aznalcazar. Obtained from AEMET.

|	Enero	Febrero	Marzo	Abril	Mayo	Junio	Julio	Agosto	Septiem-bre	Octubre	Noviem-bre	Diciembre
Temperatura media (°C)	10.1	11.4	14	16.4	20.3	25	27.5	27.8	24	19.6	13.9	11.1
Temperatura min. (°C)	5.7	6.5	8.8	10.9	14.2	18.3	20.4	21	18.3	14.7	9.5	7.1
Temperatura máx. (°C)	15.3	16.9	19.6	21.9	26.3	31.7	34.7	35	30.4	25	18.8	16
Precipitación (mm)	56	52	61	60	38	9	1	3	29	77	64	80
Humedad(%)	75%	67%	64%	62%	52%	45%	41%	43%	54%	65%	69%	76%
Días lluviosos (días)	5	4	5	5	4	1	0	0	3	6	5	5
Horas de sol (horas)	6.7	7.4	8.4	9.5	11.2	12.5	12.7	11.8	10.0	8.3	7.3	6.5
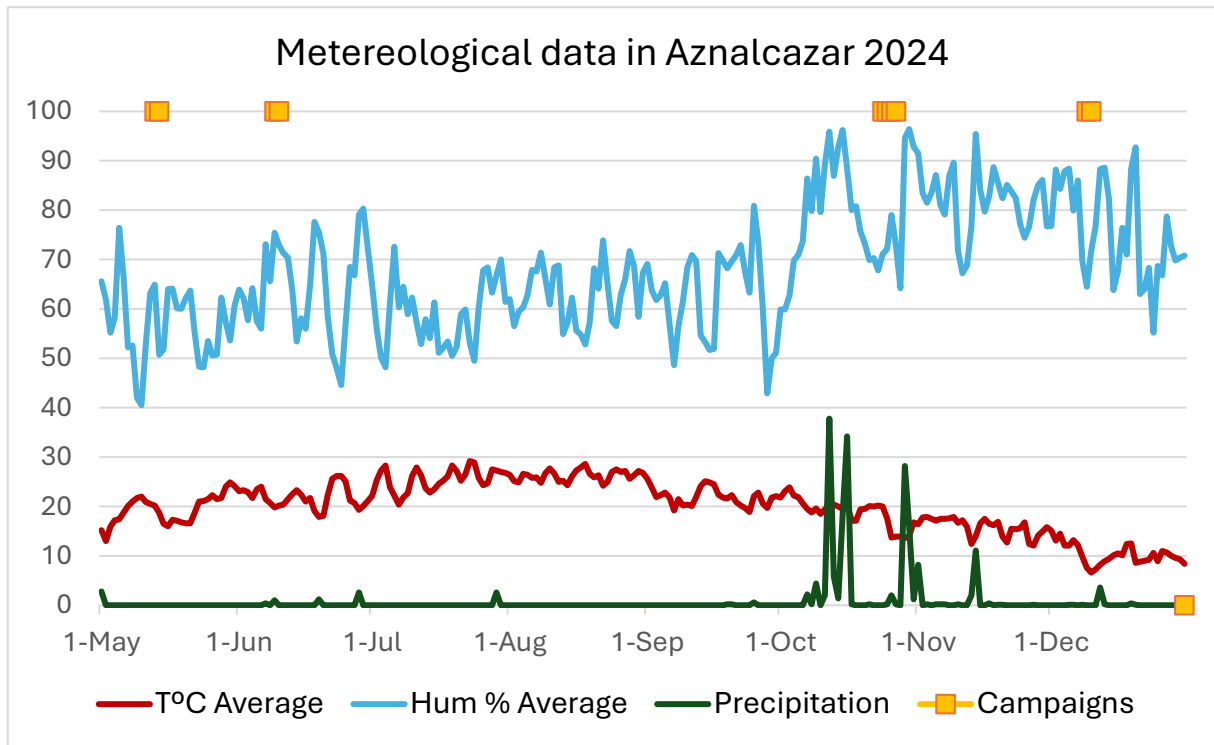
Figure 6: Meteorological data from 1st of May to 31st of December 2024. Obtained from the weather station of Aznalcazar, who records the data daily.

2.2 Instrumentation

2.2.1 CO2 flux measurements

The "accumulation chamber" method has been used to measure CO_2 fluxes from soil to the atmosphere (Elío et al., 2012; Klusman, 2011). In this method, a chamber with an open bottom is placed directly on the soil, allowing CO_2 escaping from below the surface to collect inside. The air within the chamber is circulated through a closed loop that includes an infrared detector, which measures the concentration of CO_2 (in ppm). By tracking the increase in CO_2 concentration over time [s], the rate at which CO_2 is being released from the ground is calculated (Jul et al., 2016). We have used a WEST Systems instrument, which utilizes a LICOR (LI-820) infrared detector.

The measured slope (ppm s^{-1}) measured in the field is first converted to CO_2 flux (ml min^{-1}) based on a calibration curve carried out before the fieldwork in the lab. Then, we consider the geometry of the accumulation chamber, and the pressure and temperature to convert the flux to g m^{-2} d^{-1} with the following formula:

$$\Phi\left[\frac{g}{m^2 \cdot d}\right] = \frac{dC}{dt}\left[\frac{ml}{min}\right] \cdot \frac{1}{1000}\left[\frac{l}{ml}\right] \cdot \frac{1440}{1}\left[\frac{min}{d}\right] \cdot \frac{1}{A}\left[\frac{1}{m^2}\right] \cdot \frac{P[bar] \cdot PM\left[\frac{g}{mol}\right]}{R\left[\frac{bar \cdot l}{K \cdot mol}\right] \cdot T[K]}$$

where dC/dt is the gradient of the curve of concentration versus time obtained from the calibration curve, A [m^2] the area of the accumulation chamber (0.0314 m^2), P [bar] the atmospheric pressure, PM the molecular weight of the gas (for CO_2 = 44 g mol^{-1}), R the constant of the ideal gases (0.08314510 bar l K^{-1} mol^{-1}) and T \[K\] the air temperature.

2.2.2 Soil gas measurements

Soil gas samples has been measured by mean of a portable gas chromatograph, i.e., VARIAN 490-GC QUAD model with three modules. Each analytical module functions as a miniature gas chromatograph, incorporating an injector, pneumatic system, column, and detector. All modules have TCD detectors, while the columns vary between them: i.e., with two channels having Mol Sieve 5A PLOT Capillary column (20 m x 0.32 mm), and one channel a PORAPLOT Q capillarity column (10 m x 0.15 mm). as carrier gases we use He and Ar. We measured He, Ne, H_2, O_2, Ar, N_2, CH_4, and H_2O.

The sampling is carried out using the "lost tip" method, in which a hollow rod is inserted with a pointed tip to a depth of 1 meter, that is later released by inserting a thinner rod inside the hollow one. From each sampling point, 3/4 liter of soil gas is pumped into a hermetically sealed 1-liter Teflon bag after the purge of the hollow rod to be sure that the sample is representative of the soil gas and not a mix with atmospheric air. The bags collected in the field are later transported to the lab and measured in the same day. Four samples of each bag are measured in the chromatogram, and the resultant value of the gas concentrations in a point are the average concentrations.

2.2.3 Other variables

Temperature, rainfall, and humidity data was registered from official meteorological sites and cross-checked with hourly data from the Aznalcázar weather station (*Datos de la estación | Instituto de Investigación y Formación Agraria y Pesquera (IFAPA)*, s. f.) The distance to the nearest tree was measured with a technical meter to assess the influence of roots or plant respiration on soil respiration, focusing on olive orchards. Relevant data was documented in a field notebook, including soil tillage intensity, whether the measure was taken on row or inter-row, vegetation soil cover percentage (%), including live and dead organic matter—live, such as herbaceous plants, and dead, such as dry leaves and roots—both of which can be factors influencing the rate of CO_2. or other special characteristics.

Temperature was recorded hourly, while moisture and accumulated rainfall were measured daily, resulting in a smaller dataset for these variables. Additionally, distance to the closest tree was only measured at row points, as inter-row sites in extensive orchards were considered too far for olive roots to significantly influence Rs. Ground vegetation cover was recorded within a single campaign, using one approximation per land use type.

Additionally, as a complementary study, we analyzed 4 soil samples, with mixed soil from different extraction points from the strata within the study area: i.e., pine forest, riverbank, extensive cultivation, and intensive cultivation. Soil samples were collected using a 1.5-meter auger at 0.25 m depth, except for the pine forest, where the sample were collected at 0.4 m due to the greater depth of its roots. These samples were stored in airtight plastic bags and carried out for analysis at the AGRAMA soil laboratory. The analysis focused on the percentage of organic matter, the carbon-to-nitrogen ratio (C:N), conductivity, pH, moisture content, as well as soil granulometry and texture. This campaign was conducted entirely on December 11, 2024.

2.3 Fieldwork

In total five campaigns were carried out in the area, four for the establishment the CO_2 superficial flux baseline (C1 - May, C2 - June, C3 - October, and C4 - December 2024, with 77, 79 , 211, 150 measurement points respectively) and one for soil gas measurements (C5 - July 2024 with 10 measurement points). The main objectives of these campaigns were: i) to establish the baseline CO_2 flux and the seasonal variability of CO_2 flux, 2) to evaluate the gas compositions at the subsurface, and 3) to study the influence of land use variability in the CO_2.

For the data analysis, C1 and C2 were merged because they were conducted in close temporal proximity and they may represent the summer conditions in the area, while C3 was in autumn, and C4 in winter. Furthermore, **C1** only included extensive olive grove measurements, while **C2** covered all strata except for the extensive olive grove. Therefore, by combining them, we ensure that all campaigns cover all land-use types presented in the study area, making the datasets comparable.

The sampling methodology for biological respiration monitoring campaigns was planned as follows (Figure 7: i) take measurements in a dense, regular sampling grid (e.g.

approx. 25 m between sampling points) to obtain a comprehensive and robust baseline in the footprint, with a particular focus on the well reservoir, which corresponds to the extensively managed olive grove. ii) a simple random sampling in the remaining strata to capture the widest possible spatial variability and diversity of soil types. On the other hand, due to fact that the gas chromatograph measurements requiring significantly more time and materials, air samples were collected from 10 different points (Figure 8, Table 6). Six of these were taken within the Palancares footprint, while the remaining four were taken around nearby wells from other reservoirs, some of which are almost depleted (7,8,10) and others still in active extraction (9). This was done to investigate potential micro-seepages in nearby wells. Besides, we conducted an experiment in which the same two points in the pine forest were measured four times throughout the day to study daily variability.
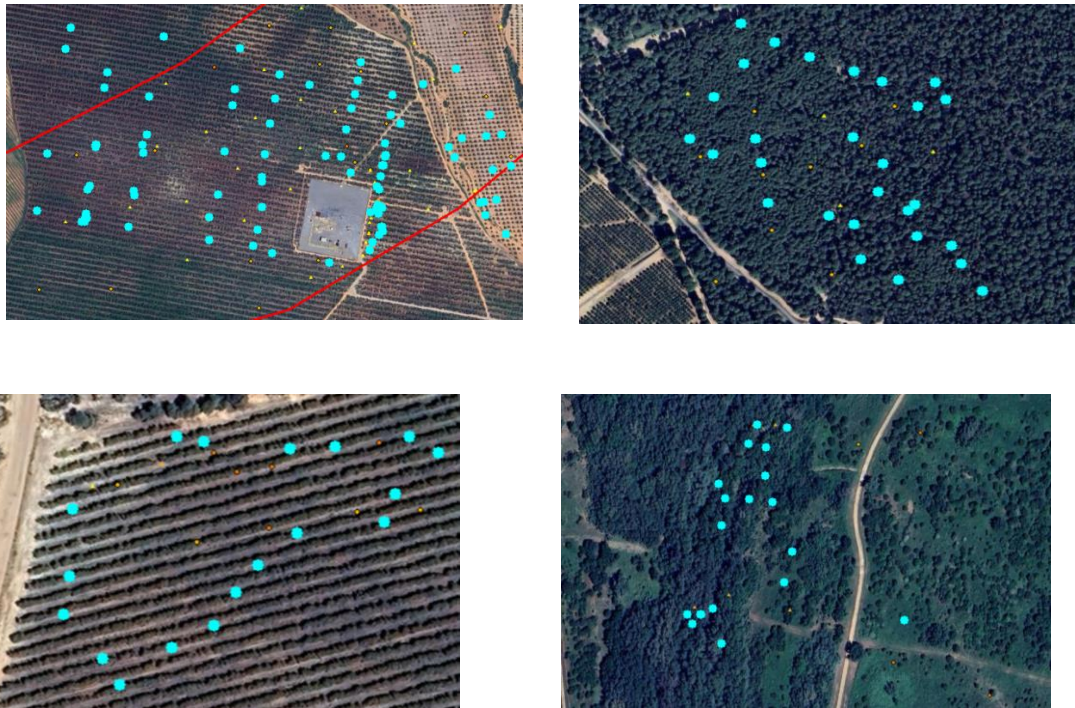

Figure 7: Example of sampling strategies a) Regular grid sampling design, Palancares well (C3, scale 1:6000), b) Random sampling design, pine forest.(C2, scale 1:6000), c) Random sampling design, Intensive Olive grove (C2, scale 1:1000), and Random sampling design, Guadiamar river corridor (C2, scale 1:2500)

Figure 8: Gas chromatography campaign measurement points.

Soil respiration measurements were performed mainly between 9:00 and 12:00 (solar time), although in most campaigns, fieldwork extended until midday. In each sampling unit, the following data were recorded both manually and digitally: i) CO_2 flux measurement, ii) air temperature, iii) proximity to the nearest tree, iv) whether the measure is row or inter-row, v) level of soil vegetation cover, and vi) relevant notes within the stratum.

Figure 9: Soil respiration measurement procedure.

2.4 Statistical analysis

Linear mixed-effects models (Bates et al., 2015) were implemented in R to analyze the relationship between CO_2 flux (response variable) and the predictors: land use, distance to the nearest tree, street/intersection, temperature, humidity, vegetation cover, and accumulated precipitation (1 month). A random effect was included to account for pseudo-replication. Model assumptions were thoroughly evaluated: residuals were tested and confirmed to meet the assumption of normality, homoscedasticity was verified through residual plots, and no evidence of multicollinearity among predictors was detected. These checks ensured the robustness and validity of the analysis.

M1: (FLUJO ~ SUELO + (1|CAMP))

M2: (FLUJO ~ CANOPY + (1|CAMP/SUELO))

M3: (FLUJO ~ ARBOL + (1|CAMP/SUELO))

M4: (FLUJO ~ TEM + HUM + PREC + COB + (1|CAMP:SUELO))

We used four linear mixed models to analyze different aspects of CO_2 flux variation. M1 examines differences in flux across land uses. M2 assesses variations between measurements taken in the row or inter-row within agricultural fields. M3 evaluates how flux changes with distance from the tree in cultivated areas. Finally, M4 captures the effect of seasonality on CO_2 flux, considering air humidity, temperature, accumulated rainfall, and vegetative soil cover. We used mixed models to include CAMP:SUELO as a random effect, accounting for pseudo-replication, since multiple measurements were taken under the same conditions within each soil type.

R scripts, as well as the campaign dataset containing all variables, can be found here: https://github.com/Mikelanies17/Soil-respiration-variability.git

3.Results

3.1 Soil respiration

Table 3: statistical data of the three-soil respiration campaigns.

campaign	points	mean	sd	min	max	season
1	153	8.03	8.75	1.06	55.2	spring-summer
2	209	11.42	7.65	1.94	72.29	autumn
3	148	7.47	4.35	1.1	29.41	winter

The table 3 presents CO_2 flux measurements grouped by three campaigns, corresponding to spring-summer, autumn, and winter. Autumn (C2) has the highest mean flux (11.42) and the widest range (1.94 to 72.29), indicating high variability, while spring-summer (1) shows a lower mean (8.03) but the highest standard deviation (8.75), suggesting a wide spread of values. Winter (3) has the lowest mean (7.47) and the smallest variability (sd = 4.35), with a much lower maximum value (29.41) compared to the other seasons.

Table 4: Summary statistics of soil respiraton measurements by land use type

land use	count	mean	sd	min	max
SE_EX almond orchard	34	5.5 g/m^2d	2.32	1.32	11.67
SE_EX olive orchard	61	8.1 g/m^2d	10.01	1.16	72.3
EX olive orchard	229	8.3 g/m^2d	5.47	1.06	52.84
IN olive orchard	56	7.4 g/m^2d	4.48	1.11	21.26
Pine forest	71	9 g/m^2d	4.36	2.47	23.43
Guadiamar riverland	59	18.3 g/m^2d	11.01	5.28	55.2

The table presents CO_2 flux measurements grouped by the different land uses. Guadiamar riverland has the highest mean flux (18.3 g/m²·d) and variability (sd = 11.01). Pine forest also has a relatively high mean flux (9 g/m²·d), but with low variability. Olive groves show intermediate values, with extensive olive grove (8.3 g/m²·d) having the highest flux among them, while semi-extensive olive grove (8.1 g/m²·d) displays the greatest variability (sd = 10.01). Intensive olive grove (7.4 g/m²·d) presents a slightly lower flux with moderate variation. Semi-extensive almond grove has the lowest mean flux (5.5 g/m²·d) and the narrowest range, suggesting more stable values. In terms of sample points, most land uses have a similar number of measurement points (ranging from 34 to 71), except for extensive olive grove, which has significantly more (229).
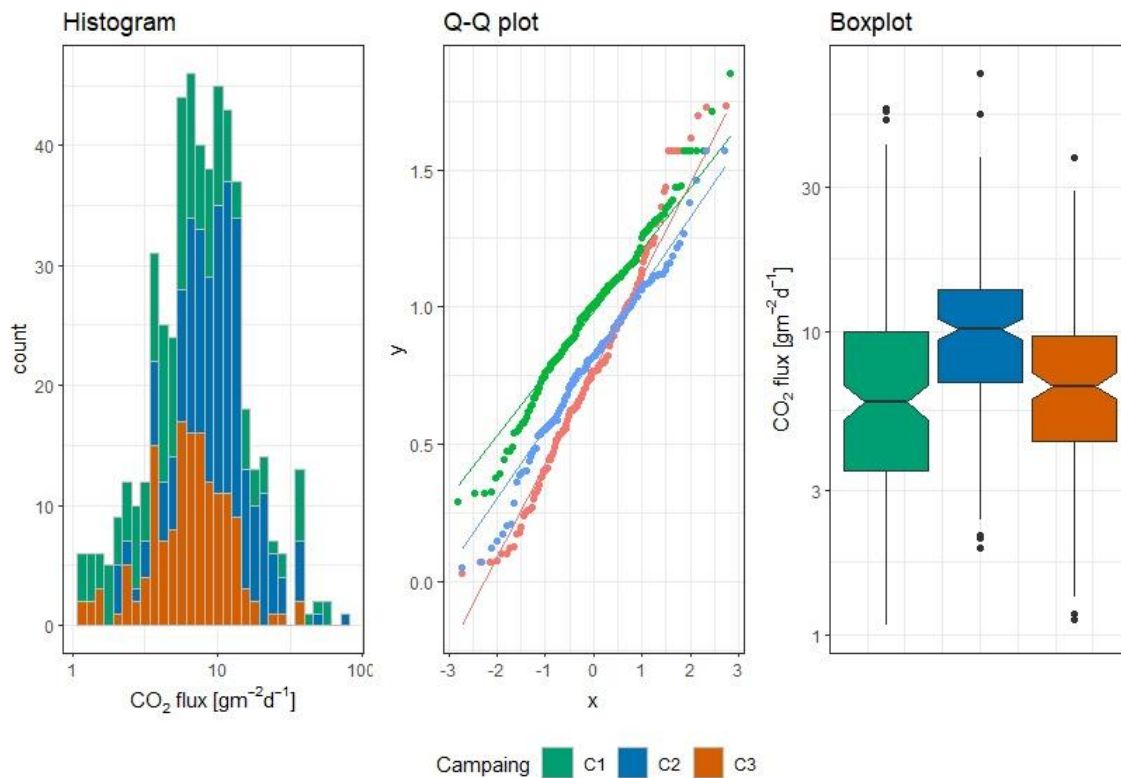
Figure 10: Distribution of CO2 flux values [in g m^-2 d^-1] after imputing values below the detection limit(<1g/m2d).

In (Fig 10) the soil respiration values are represented after imputing values below detection limit (<1g/m2d). In the histogram (left panel), CO_2 flux values are shown on a logarithmic scale, with most data concentrated between 3 and 10 g m^{-2} d^{-1}. The three campaigns follow a similar pattern, though C3 (orange) has slightly lower frequencies in the mid-range. The distribution is slightly right skewed, but overall, it resembles a normal distribution. The Q-Q plot (middle panel) assesses normality by comparing observed quantiles with a theoretical normal distribution. The points mostly align with the diagonal, though some deviations appear at the extremes, suggesting minor departures from normality due to outliers. The boxplot (right panel) shows that C2 has the highest median, followed by C3, while C1 has the lowest. The spread of values is similar across campaigns, though C1 appears slightly more compressed. All three have some high outliers, consistent with the slight right-skewness observed in the other plots. Despite this, the distributions remain practically normal.
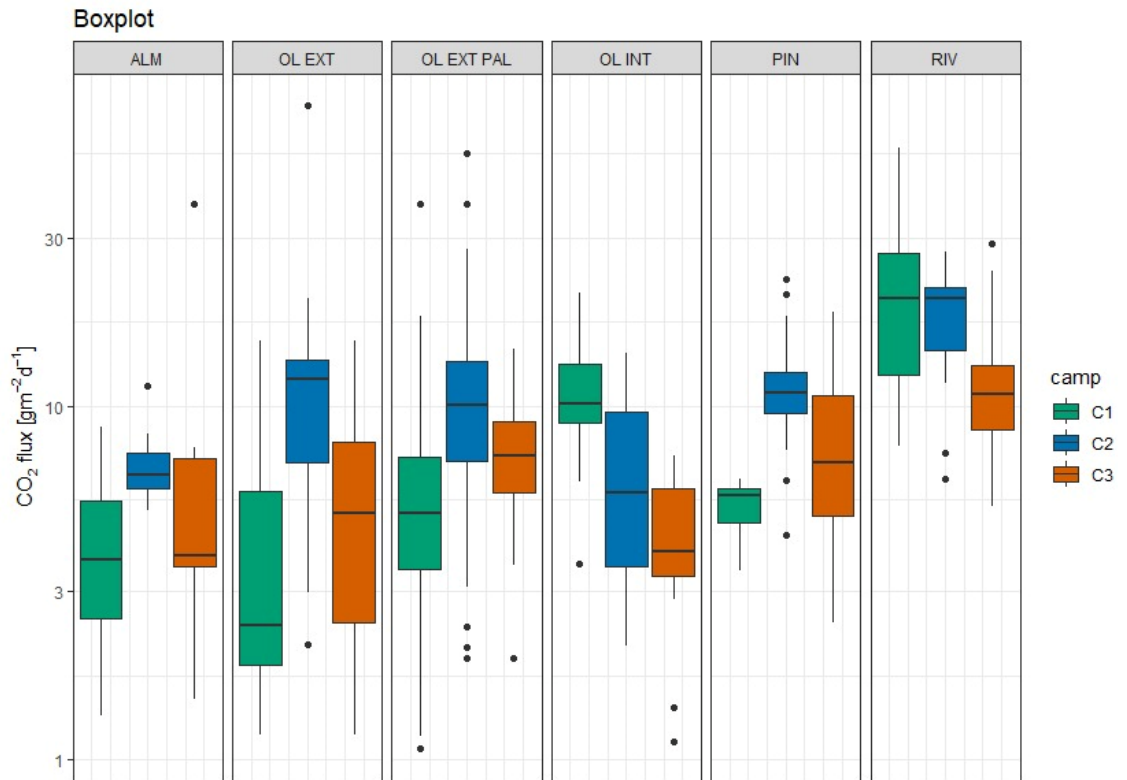
Figure 11: CO2 fluxes distributed by soil types and by campaign.

The boxplot (Figure 11) shows the variation in soil CO_2 flux across different land-use types over three seasonal campaigns: spring-summer (C1), autumn (C2), and winter (C3). A consistent pattern emerges in most soils: C2 (Autumn) has the highest median values, followed by C3 (Winter), with C1 (Spring-Summer) being the lowest. This trend is visible in almond orchard, extensive olive grove, semi-extensive olive grove, and pine forest. However, two soils deviate from this pattern: riverbank and intensive olive grove, where C1 (Spring-Summer) has the highest CO_2 flux, followed by C2 (Autumn), with C3 (Winter) being the lowest. Three general trends can be observed: riverbank (RIV) consistently exhibits the highest respiration rates, pine forest (PIN) and olive groves (OL EXT, OL EXT PAL, OL INT) show intermediate values, while almond (ALM) remains consistently lower than the other land uses.
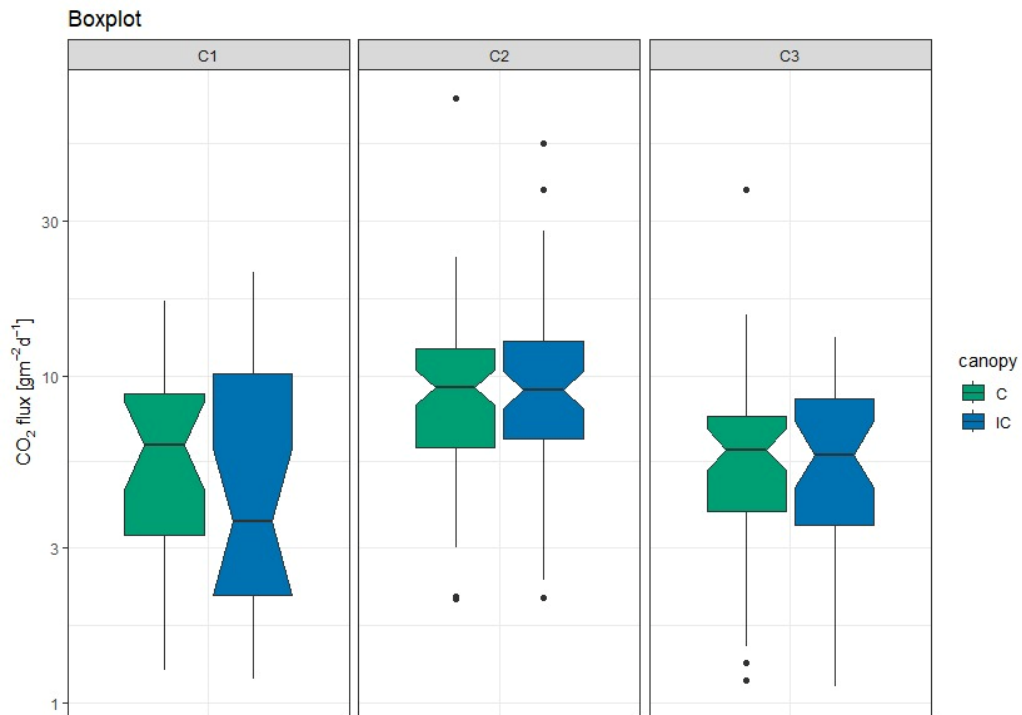
21

Figure 12: Under-canopy or inter-canopy Rs estimated values grouped by campaigns. (C1: spring-summer, C2: autumn, C3: winter) under canopy (C) and inter-canopy (IC) conditions.

This boxplot shows soil CO_2 flux across three campaigns and under canopy (C) and inter-canopy (IC) conditions. In C1, fluxes have the highest variability, with noticeable differences between C and IC, being C approximately 2 g higher than IC. In C2, values are more uniform, with no apparent differences between C and IC. In C3, fluxes are lowest, with minimal differences between canopy conditions. The differences between C and IC are more pronounced in warmer conditions, while in colder seasons, respiration rates become more homogeneous and no difference between site occur.
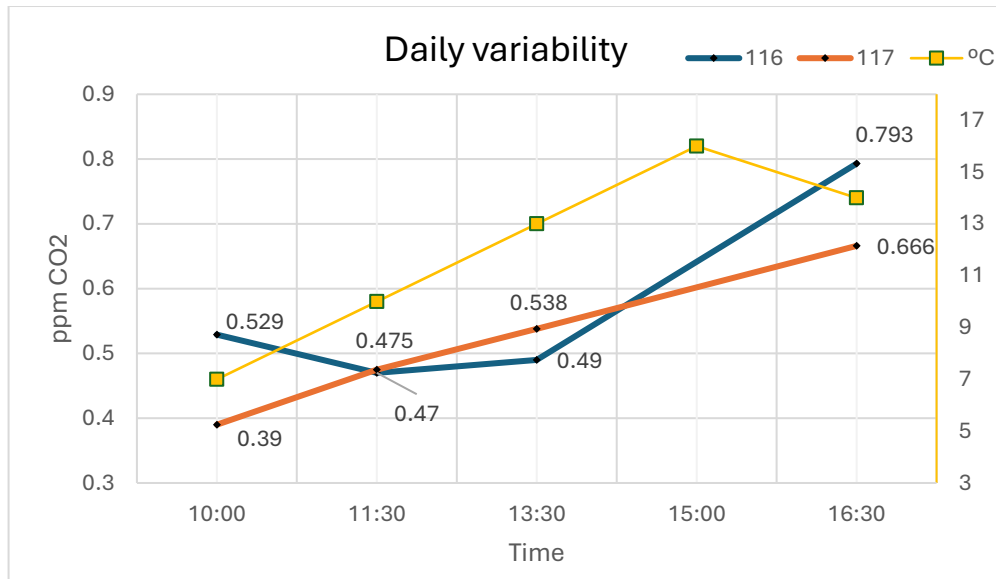
Figure 13: Daily variability studied in two measurements point within the pine forest strata which were measured at four different times during the C4.

The graph. shows soil respiration measurements (CO_2 flux in ppm) at two points (116 and 117) taken at different times of the day, along with temperature variations (°C). CO_2 levels gradually increase throughout the day at both points, with 116 showing slightly higher values than 117, especially in the afternoon. Temperature follows a similar pattern, rising until 15:00 before slightly decreasing at 16:30.
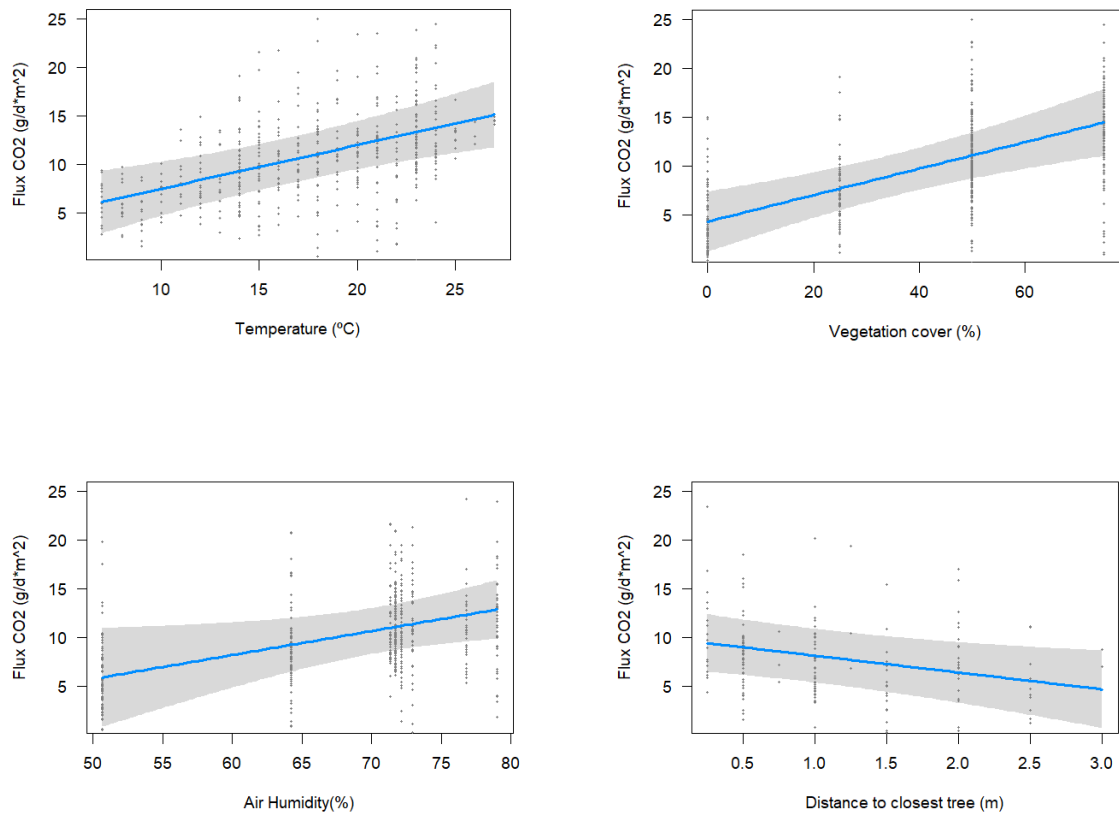
Figure 14: Representation of the significant predictor variables (X) in relation to the response variable Rs (Y). Arranged from top to bottom and from left to right: (A) air temperature,(B) ground vegetation cover,(C) air humidity, and (D) distance to the tree.

Temperature is plotted against CO_2 flux (A), with the X-axis spanning from 5°C to 27°C. It shows a steady increase in CO_2 flux as temperature rises, with mean values moving from around 7 g/dm² at 10°C to approximately 15 g/dm² at 25°C. The data points are widely spread but generally follow the upward trend indicated by the regression line. CO_2 flux is plotted against vegetation cover (B), with the X-axis ranging from 0% to 75%. The blue line indicates a clear upward trend as the vegetation cover increases, with the mean flux rising from approximately 5 g/dm² at 0% to around 14 g/dm² at 75%. Data points are widely spread along the range, with some higher densities of points observed at lower vegetation cover percentages.

Air humidity is plotted against CO_2 flux, with the X-axis covering a range from 50% to 80%. It shows a gradual increase in CO_2 flux as humidity rises, with mean flux values moving from around 8 g/dm² at 50% humidity to approximately 13 g/dm² at 80%. The data points are relatively dispersed, particularly at higher humidity. Distance to the closest tree is plotted against CO_2 flux, with the X-axis covering a range from 0.25 m to 3 m. The blue line shows a slight negative trend, with CO_2 flux decreasing from around

8 g/dm² at shorter distances to approximately 6 g/dm² at 3 m. The data points are more densely concentrated at shorter distances and become more scattered as the distance increases.
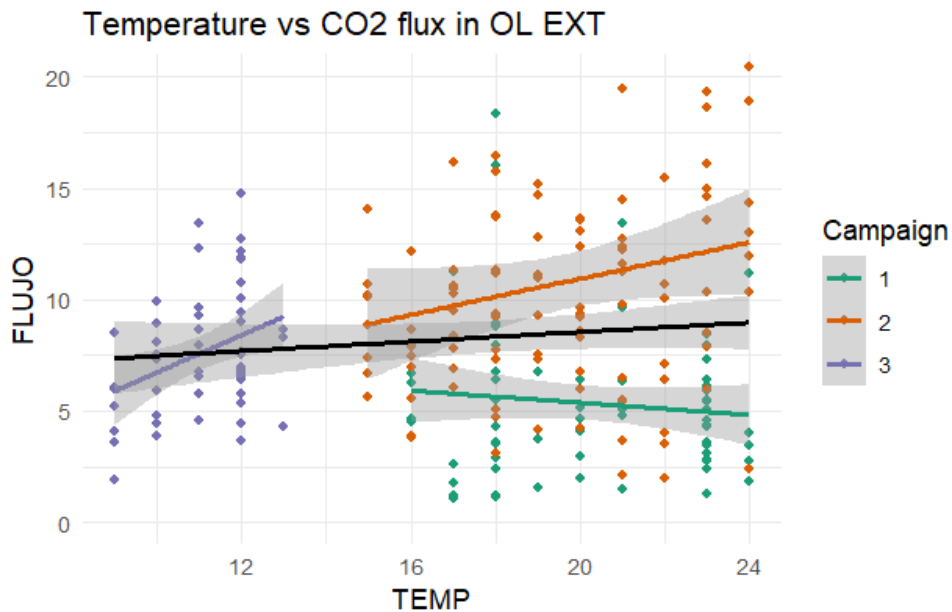

Figure 15: relationship between temperature and soil CO_2 flux in the extensive olive grove across campaigns: summer (C1), autumn (C2), and winter (C3).

Data points are scattered across the temperature range, showing variability in CO_2 flux among seasons. In autumn and winter, a positive trend is observed, where CO_2 flux increases with temperature. The winter trend line has a slightly steeper slope compared to autumn. Winter data is also more concentrated at lower temperatures, with a more dispersed pattern. In contrast, summer shows a negative trend, where CO_2 flux decreases as temperature rises. Trend lines for each season highlight these differences, with narrower confidence intervals in autumn and wider intervals in summer and winter.

predictor variable	intercept	error	pr(>F)	Signification
Land use	4.949	1.712	2.2E-16	***
Row / Inter-row	-0.455	0.589	0.4395	
Tree distance	-1.594	0.571	0.00561	**
Coberture	0.136	0.033	0.0008971	***
Temperature	0.451	0.119	0.0002436	***
Air humidity	0.247	0.115	0.0374	*
Cumulative precipitation	0.033	0.020	0.1135	

Table 5 & 6: Results of the linear-mixed models

Variable	M1	M2	M3	M4
Random Effects				
CAMP	5.156	2.341	3.789	
SUELO:CAMP		7.619	4.049	13.71
Fixed effects				
(intercept)				
Land use	4.949 (2^{-16}) ***			
Row/inter-row		-0.4554 (0.4395)		
Tree distance			-1.594 (0.0056)**	
Vegetative coverture				0.136 (0.0009) ***
Temperature				0.451 (0.00024) ***
Air humidity				0.247 (0.0374) *
Cumulative precipitation				0.331 (0.019)

The table presents a statistical analysis of predictor variables influencing soil respiration (Rs), showing that land use, soil vegetative cover, and temperature are highly significant ($p < 0.001$), while tree distance and air humidity have moderate significance ($p < 0.05$), whereas row/Inter-row and cumulative precipitation are not statistically significant ($p > 0.05$). The intercept values indicate the estimated baseline effect of each predictor, with associated errors reflecting variability.

3.2 Gas chromatography

Table 6: Soil gas concentrations (in ppm) measured by gas chromatography.

ID	lat	long	He	Ne	H2	O2	N2	CH4	CO2	H2O
1	37.31826	-6.206419	1.950	0	0	142067.7	784054.8	13.200	9337.075	0
2	37.31791	-6.206922	1.975	0	0	145988.9	784352.5	10.650	7164.375	0
3	37.32125	-6.205276	1.975	0	0	143561.1	784878.5	10.900	10420.725	0
4	37.32078	-6.204974	2.000	0	0	172464.5	795494.3	9.875	2271.975	0
5	37.31431	-6.226523	2.025	0	0	136553.1	780190.2	13.225	13717.175	0
6	37.31543	-6.226946	2.000	0	0	146962.9	787738.1	12.750	7924.925	0
7	37.27431	-6.271242	0.000	0	0	129788.2	769639.3	18.050	28467.850	0
8	37.26091	-6.286147	0.000	0	0	137233.3	776987.9	18.225	17805.150	0
9	37.27347	-6.297989	0.000	0	0	130424.8	771221.6	22.175	25904.800	0
10	37.33202	-6.168153	1.475	0	0	140331.7	782188.9	14.425	10045.050	0

The gas chromatography analysis conducted at a depth of 1 meter across ten different points shows relatively consistent results (Table 5).), with common gas concentrations that suggest a natural origin . Oxygen (O_2) and nitrogen (N_2) are the most abundant gases, with O_2 ranging from approximately 130,000 to 172,000 ppm and N_2 between 770,000 and 795,000 ppm. Methane (CH_4) and carbon dioxide (CO_2) are present in lower concentrations, with CH_4 values between 9.9 and 22.2 ppm and CO_2 ranging from 2,300 to 28,500 ppm. In contrast, helium (He) appears in very low concentrations, while neon (Ne) and hydrogen (H_2) were not detected. This absence may probably be due to their concentrations being below the detection limit of the equipment used. Water vapor (H_2O) is also undetectable across all measurements.
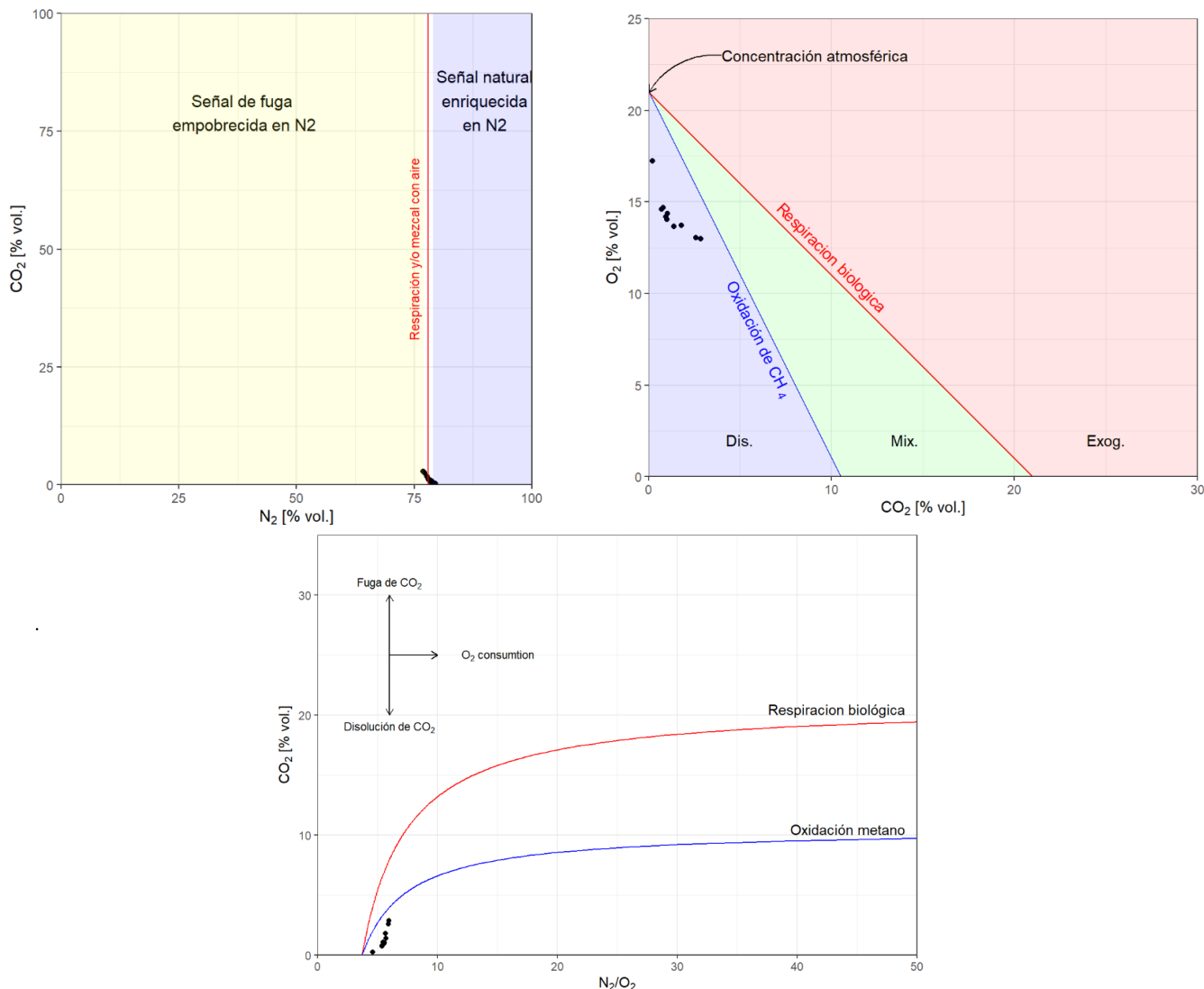
Figure 16: Geochemical relationship in soil gas between a) CO₂ [%] and O₂ [%], b)CO₂ [%] and N₂ [%], and c) CO₂ [%] and the N₂/O₂ [%] ratio

The CO_2 vs. O_2 plot, based on gas chromatography measurements, shows that the sampled points are distributed within the dissolution and mixed regions of the graph. Most values exhibit a negative correlation between CO_2 and O_2, aligning with the expected trend for biological respiration. No data points fall within the exogenous CO_2 zone. Given this distribution, there is no evidence of deep gas leaks. The CO_2 concentrations observed are consistent with soil respiration and dissolution in rainwater, as indicated by their positioning in the graph.

The N_2 vs. CO_2 graph, based on gas chromatography measurements, shows that the sampled points are closely aligned with the vertical line representing atmospheric nitrogen concentration. No data points fall within the N_2-depleted leak signal zone. This pattern is consistent with a biological origin of CO_2 in soil gas, with no detectable contribution from the storage reservoir. If such a contribution were present, samples would be expected to appear further to the left of the atmospheric N_2 reference line.

The N_2/O_2 vs. CO_2 graph, based on gas chromatography data, shows that the sampled points are clustered in the lower left region. This distribution aligns with values expected for carbonate dissolution and microbial respiration. No points appear in the

28

upper regions associated with methane oxidation or strong biological respiration. According to (Romanak et al., 2012), the N_2/O_2 ratio helps distinguish methane oxidation from microbial respiration and carbonate dissolution. The results in this study follow this pattern, supporting a natural origin for the detected CO_2.

3.3 Soil analysis results

Table 7: Results of the analysis of the soil samples from the different strata

AMBIENTE	Arcilla %	Arena %	Limo %	Textura USDA	Cond µS/cm	MOT %	PH	N%	HUMEDAD%
Rivera	10	49	41	Franco	120	1.25	8.7	0.095	14.4
Pinar	5	80	15	Areno-limoso	<50	0.41	7.8	0.029	9.65
Olivar extensivo	15	62	23	ranco-arenos	64.5	1.13	8.9	0.1	8.45
Olivar intensivo	20	51	29	Franco	130	0.81	8.9	0.089	11.1

The analyzed soils show variations in texture, composition, and certain physicochemical properties. The four environments present different soil textures: riverbank and intensive olive grove are classified as loam, pine forest as sandy silt loam, and extensive olive grove as sandy loam. The sand content ranges from 49% to 80%, with pine forest having the highest proportion, while the clay content varies between 5% and 20%, being lowest in Pine forest and highest in Intensive olive grove. The silt content also varies, with the highest percentage in riverbank (41%) and the lowest in extensive olive grove (23%). The pH values are consistently basic, ranging from 7.8 to 8.9, which suggests conditions favorable for many crops but potentially limiting nutrient availability in some cases. Electrical conductivity remains low (<50–130 µS/cm), indicating minimal salinity. Organic matter (MOT%) is highest in riverbank (1.25%) and lowest in pine forest (0.41%), showing variations across the environments. The total nitrogen content is generally low, with values between 0.029% and 0.1%. Soil moisture also differs among environments, with the highest percentage in riverbank (14.4%) and the lowest in extensive olive grove (8.45%).

Discussion

Soil respiration baseline

Daily, seasonal, and spatial variability were all observed in the study. Rs values increases as the day progresses (Figure 13), which appears to be directly related to rising temperatures. CO_2 flux significantly decreases during the early morning hours and increases throughout the day, reaching up to 1.6 times the measured flux between 10:00 and 16:00, as shown in our figure. This pattern is consistent with findings from other studies in Mediterranean systems, where mid-morning CO_2 efflux values (9:00–12:00) have been shown to be representative of daily averages (Almagro et al., 2009), and a peak in soil respiration was observed at 15:00 across all seasons and for both row and inter-row positions (Lardo et al., 2015a). However, we cannot rule out the influence of other factors, such as moisture and substrate availability, which exhibit distinct temporal and spatial patterns.

In semi-arid regions, while soil temperature is a primary driver of CO_2 emissions, its effect is modulated by moisture levels, making traditional Rs models—primarily based on temperature and designed for temperate climates—less applicable to Mediterranean environments (Aranda-Barranco et al., 2024; Lardo et al., 2015a; Lei et al., 2021). In these ecosystems, soil temperature and moisture are strongly correlated, meaning that their combined influence must be considered when assessing Rs dynamics (Almagro et al., 2009; Maestre & Cortina, 2003). As demonstrated in a previous study, these two variables served as effective predictors in a simple and efficient conditional model, explaining approximately 84% of the total annual variance in Rs (Montanaro et al., 2023). For this reason, our model (m4) incorporates air humidity, cumulative precipitation, and temperature to account for their combined influence on Rs dynamics ($R^2=0.5$).

Both temperature and soil moisture were significant factors, whereas cumulative precipitation was not (Table 5). Temperature shows greater significance, which may be attributed to small dataset of moisture and accumulated rainfall variables. Rs showed a clear positive correlation with temperature, consistent with previous studies (Figure 14). Moreover, to analyze seasonal variability, we focused on a single land use type— the extensive olive orchard—as it had the most sampling points, allowing us to keep multiple variables stable and facilitating the establishment of relationships between variables. When examining Rs trends across campaigns, distinct seasonal patterns emerged (Figure 15). In autumn and winter, Rs increased with temperature, with winter showing a stronger slope and much colder conditions. In these ecosystems, Rs typically increases with temperature when moisture is not limiting, which didn't occur due to the high moisture levels (in autumn campaign, soil moisture was 70.5% with 108.4 mm of accumulated rainfall, and in winter, it reached 73% with 14.1 mm of rainfall).

However, during drought periods soil moisture restricts decomposition processes and leads to a decrease in Rs despite rising temperatures (Montanaro et al., 2023), as observed in a study of a Mediterranean steppe (Bertolla et al., 2014). This could explain what occurred in the spring-summer campaign, which the trend was negative but less pronounced than others, indicating an inverse relationship between Rs and temperature under high-temperature conditions. June temperatures were not particularly high

compared to typical values for the region during this period, reaching a maximum of 27°C, 3°C higher than the peak temperature recorded in the autumn campaign. Additionally, air humidity was lower (61.7%), and no significant rainfall (3.3) had occurred since April (Figure 6).

Furthermore, other explanation to this negative correlation in the warmest campaign could be found in the fact that even when moisture is available, Rs does not increase indefinitely with temperature; above a certain threshold, co-occurring limitations such as substrate availability and microbial biomass limit further CO_2 release (Aranda-Barranco et al., 2024). A study in an irrigated olive orchard in Jaen, support this threshold-based behavior, showing a decline in Rs when soil temperature exceeds a critical value, even with stable soil water content (<20%). A negative correlation between Rs and temperatures above 20°C has been observed, suggesting that this threshold-based approach could be applied to various Mediterranean olive ecosystems (Chamizo et al., 2017). Even with irrigation, if the temperature exceeds the threshold, it has been observed that Rs did not increase (Montanaro et al., 2023). In addition, this may also explain why the correlation line slope for the winter campaign is the steepest, as temperatures in the autumn campaign (up to 24 ºC) exceeded the assumed 20°C threshold.

Our data show a peak in Rs during the autumn campaign (C2), followed by lower values in summer (C1) and reaching minimum values in winter (C3) (Table 3), aligning with previous studies that report Rs peaks in spring and autumn in Mediterranean climates (Almagro et al., 2009; Aranda-Barranco et al., 2024; Lardo et al., 2015a; Salinas Alcantara, 2018). In this regard, (Almagro et al., 2009) proposed dividing the year into a 'growing' season (October–April) and a 'dry' season (May–September), a pattern further supported by (Montanaro et al., 2023) who found that higher root density and bacterial biomass in the row position contributed to total soil respiration (TSR) mainly during the growing season. The seasonal pattern we observe in our data can be, therefore, explained by moderately high temperatures and elevated moisture levels during autumn, whereas winter values remain the lowest due to colder temperatures and low biological activity (7-14ºC). Summer Rs declines due to moisture limitation, temperature thresholds, and the absence of prior rainfall.

Spatial variability was quantified with the different land uses, vegetative cover soil proportion, distance to the closest tree, and whether the measurement was carried out on row or inter-row, also called as under-canopy and inter-canopy. The land use variable was significant (Table 5); however, Tukey tests and pairwise comparisons revealed that significant differences were only found between the riverbank, and the other land use types. The highest Rs values were recorded in the riverbank and pine forest areas, which is unsurprising given that, as forested areas, they are more naturalized, with greater soil development, increased vegetation density, and a greater root concentration. The riverbank had the highest Rs, likely due to its shallow water table, which supports greater tree density and ground vegetation cover, higher soil moisture, and increased organic matter content (Table 7). This is further influenced by the alluvial soil, where sediment deposition from typical Mediterranean floods enhances fertility and carbon accumulation. A similar pattern was observed in a previous study comparing a forested ecosystem with an irrigated olive orchard, where Rs levels in the forest were slightly higher than those measured in the olive grove (Almagro et al., 2009).

All land uses reached their maximum average Rs in autumn, except for the intensive olive orchard and riverbank, which peaked in C1 (spring-summer) (Figure 11). This can be explained by the fact that harvesting in intensive olive orchards is performed with heavy machinery, which compacts the soil, reducing air between pores. By the time we arrived for C2, the soil was highly compacted, with no visible vegetation remnants, in contrast to C1, where soil vegetation was present. In the riverbank, this pattern could be attributed to the loamy soil composition (Table 7), which has a high silt content, providing good infiltration and water retention. During autumn rains, pores may have filled with water, reducing the presence of gases in the soil. Additionally, in summer, the effect of high temperatures was evident in the characteristic pattern of expansive clay soils, which form cracks. Measurements in these soils may have overestimated Rs, as the increased air exchange between the soil and the atmosphere could have naturally inflated the flux values.

Soil analyses showed similar values across most parameters (Table 7), with low electrical conductivity, basic pH (7.8–8.9), low nitrogen content, and moisture around 10%. Organic matter content ranged from 1.25% in the riverbank to 0.41% in the pine forest, with intermediate values of 0.81% in intensive olive groves and 1.13% in extensive ones. These values align with previous findings, where average organic carbon levels in olive groves were reported at $1.58 \pm 0.71\%$, tending to be lower in tilled than in grazed systems (Álvarez et al., 2007). Soils with higher organic matter store more carbon, while sandy soils (Pine forest) have lower storage capacity than clay-rich soils, which retain more moisture (Rutgers et al., 2016). A balance between drainage (sand) and moisture retention (silt and clay) is shown in both orchards (Table 7), explaining the traditional establishment of olive groves in Aljarafe, where soil moisture supports tree survival and olive growth even during summer droughts, allowing harvest in September.

Regarding crop intensification, average Rs values, though similar in magnitude, showed notable differences (Table 4). Extensive and semi-extensive olive groves had the highest Rs (8.3 and 8.1, respectively), followed by intensive olive groves (7.4) and semi-extensive almond orchards (5.5). One key factor may be the age of the plantations, as the first two date back to before 1986, while the others were established in 2018 and 2020. Older plantations contribute to greater Rs due to the greater root density. Furthermore, it has shown orchards has positive effects on soil fertility and boost the abundance and biomass of soil (micro)biota in long term (25y)(Kooch et al., 2023; Martin-Gorriz et al., 2020).

High Rs is expected in modern agricultural systems due to the use of fertilizers, irrigation, and soil aeration, greater carbon inputs also enhance soil fertility by improving water retention, porosity, and stability, while simultaneously increasing microbial activity and decomposition rates. Although extensive management is considered more sustainable, with manual fruit harvesting, greater natural vegetation cover in the alleys, and a wider planting framework, it resulted in slightly higher soil CO_2 emissions compared to intensive systems, which, seen without further context, could be considered controversial. However, its overall impact should be evaluated within a broader carbon balance, considering atmospheric CO_2 sequestration in different ecosystem pools (Montanaro et al., 2023). This aligns with soil analyses (Table 7), which showed higher organic matter content in extensive olive groves than in intensive ones.

Rs spatial variability is strongly influenced by vegetation distribution and plant activity (Lardo et al., 2015a). Across major biomes, a well-established relationship between soil respiration and net primary production (NPP) suggests that areas with greater vegetation cover or proximity to trees tend to show higher CO_2 emissions (Jongen et al., 2011; Raich & Schlesinger, 1992). Among our measured variables related to vegetation, distance to the tree and soil vegetative cover showed a significant positive correlation with Rs (Table 5), which aligns with expectations, as greater proximity to trees associated with higher root density, and a greater vegetation soil cover increases Rs by enhancing root respiration and microbial activity through higher organic matter input and soil moisture retention (Turrini et al., 2017). Furthermore, although all studied fields incorporated tillage methods, extensive systems allowed for greater vegetation cover, which is a more sustainable practice, preserving fertility and reducing environmental impact.

The position between row and inter-row did not show a significant effect when considering all campaigns globally, differing from similar studies (Almagro et al., 2009; Chamizo et al., 2017). However, when analyzed within each campaign and land use type, a clear pattern emerged in the summer campaign, where Rs was moderately higher in the row than in the inter-row across all soil types, while it remained practically equal during the autumn and winter campaigns (Figure 12). This summer trend only remained subtly present in the intensive olive orchard throughout the campaigns.

This could be explained due to the fact that vegetation buffers the response of soil respiration to temperature and moisture dynamics, including canopy shading, rainfall interception, and root-mediated water redistribution (Jongen et al., 2011). As a result, the influence of abiotic factors on CO_2 efflux is therefore more pronounced in open areas, whereas biotic interactions dominate beneath vegetation cover. This has been observed in studies with continuous measurements, where temperature variability on the ground was buffered near the olive tree, resulting in higher temperatures compared to the alley during cold months and lower temperatures during warmer periods (Almagro et al., 2009; Aranda-Barranco et al., 2024). The harsh summer drought conditions combined with the absence of ground cover in orchards in that season, may explain the slightly higher Rs values in rows compared to inter-rows. Grass-covered soils generally exhibit higher respiration than tilled soils due to greater labile carbon content, root density, and microbial biomass (Bertolla et al., 2014; Maestre & Cortina, 2003). This also explains the lack of difference between row and inter-row in the autumn and winter campaigns, as the progressive growth of vegetative cover throughout the year in the alleys equalizes the Rs values across the orchards.

Micro-seepage detection

The analysis of soil gas composition does not indicate the presence of deep gas leakage from the storage reservoir, as gas concentrations across all sampling points remain within the expected range for natural soil processes such as microbial respiration and carbonate dissolution. The soil respiration baseline values follow a normal distribution with natural range emissions despite the presence of some anomalous values. However, these are few, and it is more likely that they represent high values within the same population. Some of them were associated with ant nests, which appear to increase

the measured soil Rs (Caiafa et al., 2023) Establishing these gases baseline measurements is essential for future monitoring during and after hydrogen injection, providing a reference to detect potential anomalies that could arise during storage operations and ensuring reservoir integrity(Förster et al., 2006; Jul et al., 2016).

The observed gas composition follows patterns associated with biological respiration, where CO_2 increases as O_2 decreases, without deviations toward exogenous CO_2 sources (Figure 16). Similarly, the relationship between N_2 and CO_2 shows that all samples align with atmospheric N_2 levels, with no indication of N_2 depletion, which would be expected in the presence of deep gas migration. Additionally, the N_2/O_2 ratio, a key indicator for distinguishing microbial respiration and carbonate dissolution from methane oxidation (Romanak et al., 2012), follows the expected trend for biological activity rather than external CO_2 input. Furthermore, noble gases such as helium and neon, which are potential tracers for deep gas migration (Elio Medina, 2013), were either undetected or present in extremely low concentrations, further supporting the conclusion that no deep gas has reached the surface.

Conclusions

A baseline assessment of CO2 exchange, as well as other gases, has been conducted. This baseline will serve as a reference and will be used in the MMV campaigns of the pilot H2 injection project in the depleted Palancares reservoir. It would be advisable to expand the baseline with additional campaigns until the injection begins. This would provide a better understanding of seasonal variations and enhance the robustness of the study. In this study, we observed that soil respiration exhibited daily, seasonal, and spatial variability. Despite its strong correlation with soil moisture, temperature was the predictor variable that best explained seasonal variability. For future studies, soil moisture and temperature should be measured directly, and moisture values should be recorded at each sampling point to improve the model's explanatory power ($R^2 = 0.5$). Seasonal differences were observed, with the highest Rs recorded during the autumn campaign and the lowest during winter.

Land use was found to be significant, primarily due to the high Rs values observed in the riparian zone (18.3 g/m²day CO_2). No significant differences were found between different management practices in olive orchards; however, extensive olive orchards (8.3 g/m²day CO_2) showed slightly higher Rs values than intensive ones (7.4 g/m²day CO_2). In contrast, although extensive orchards exhibit higher Rs than intensive ones, the overall carbon balance must be considered. Sustainable practices such as allowing ground cover to grow freely in the alleys, reducing heavy machinery use, and wider planting spacings reduce erosion and enhance the role of soil as a carbon sink. The variables "distance to the nearest tree" and "ground vegetation cover" were also significant, whereas the position within the row (mid-row vs. inter-row) was not. Nevertheless, a difference of up to 2 g/m²day CO_2 was observed in the summer campaign, with higher values in the mid-row areas compared to the inter-rows.

While multiple points within the Palancares footprint have been measured and no signs of leakage have been detected, further monitoring is necessary to ensure the absence of micro-seepage. Additional measurements should be conducted at other locations within

the footprint during and after the injection phase. Besides, efforts should be made to improve the instrument's sensitivity to low gas levels. Furthermore, measurements taken at nearby reservoirs (Figure 8) under similar conditions also show no indications of leakage. Our results agree with what we can expect in depleted gas fields, since these reservoirs have been produced over the last decades (i.e., they are under-pressured), and have demonstrated the store capacity of gases (they have a good caprock). Therefore, these findings further reinforce the evidence that there is no micro-seepage from the reservoir.

References

Almagro, M., López, J., Querejeta, J. I., & Martínez-Mena, M. (2009). Temperature dependence of soil CO_2 efflux is strongly modulated by seasonal patterns of moisture availability in a Mediterranean ecosystem. *Soil Biology and Biochemistry*, *41*(3), 594-605. https://doi.org/10.1016/j.soilbio.2008.12.021

Al-Shafi, M., Massarweh, O., Abushaikha, A. S., & Bicer, Y. (2023). A review on underground gas storage systems: Natural gas, hydrogen and carbon sequestration. *Energy Reports*, *9*, 6251-6266. https://doi.org/10.1016/j.egyr.2023.05.236

Álvarez, S., Soriano, M. A., Landa, B. B., & Gómez, J. A. (2007). Soil properties in organic olive groves compared with that in natural areas in a mountainous landscape in southern Spain. *Soil Use and Management*, *23*(4), 404-416. https://doi.org/10.1111/j.1475-2743.2007.00104.x

Aranda-Barranco, S., Serrano-Ortiz, P., Kowalski, A. S., & Sánchez-Cañete, E. P. (2024). Spatial and temporal heterogeneity of soil respiration in a bare-soil Mediterranean olive grove. *EGUsphere*, 1-30. https://doi.org/10.5194/egusphere-2024-848

Bates, D., Mächler, M., Bolker, B., & Walker, S. (2015). Fitting Linear Mixed-Effects Models Using lme4. *Journal of Statistical Software*, *67*, 1-48. https://doi.org/10.18637/jss.v067.i01

Bertolla, C., Caruso, G., & Gucci, R. (2014). SEASONAL CHANGES IN SOIL RESPIRATION RATES IN OLIVE ORCHARDS. *Acta Horticulturae*, *1057*, 275-280. https://doi.org/10.17660/ActaHortic.2014.1057.30

Caiafa, L., Barros, N. O., & Lopes, J. F. S. (2023). Greenhouse gas emissions from ant nests: A systematic review. *Ecological Entomology*, *48*(4), 397-408. https://doi.org/10.1111/een.13238

Chamizo, S., Serrano-Ortiz, P., López-Ballesteros, A., Sánchez-Cañete, E. P., Vicente-Vicente, J. L., & Kowalski, A. S. (2017). Net ecosystem CO_2 exchange in an irrigated olive orchard of SE Spain: Influence of weed cover. *Agriculture, Ecosystems & Environment*, *239*, 51-64. https://doi.org/10.1016/j.agee.2017.01.016

Ciotta, M., & Tassinari, C. C. G. (2024). Defining geological viability criteria for CO2 and hydrogen storage in depleted oil and gas fields. *Research, Society and Development*, *13*(8), Article 8. https://doi.org/10.33448/rsd-v13i8.46130

Clima Mairena del Aljarafe: Temperatura, Climograma y Tabla climática para Mairena del Aljarafe. (s. f.). Recuperado 29 de enero de 2025, de https://es.climate-data.org/europe/espana/andalucia/mairena-del-aljarafe-57068/

Datos de la estación | Instituto de Investigación y Formación Agraria y Pesquera (IFAPA). (s. f.). Recuperado 28 de enero de 2025, de https://www.juntadeandalucia.es/agriculturaypesca/ifapa/riaweb/web/estacion/41/5

DIEGO, B. N., RICARDO, F. E., & LUIS, R. R. (2017). *El cultivo del olivo 7ª ed.* Ediciones Mundi-Prensa.

Elío, J. (2024). *Understanding hydrogen seepage in engineered reservoirs: Processes, pathways and monitoring techniques* (SSRN Scholarly Paper No. 5066329). Social Science Research Network. https://papers.ssrn.com/abstract=5066329

Elío, J., Nisi, B., Ortega, M. F., Mazadiego, L. F., Vaselli, O., & Grandia, F. (2013). CO2 soil flux baseline at the technological development plant for CO2 injection at Hontomin (Burgos, Spain). *International Journal of Greenhouse Gas Control*, *18*, 224-236. https://doi.org/10.1016/j.ijggc.2013.07.013

Elío, J., Ortega, M., Caballero, J., García, J., Nisi, B., Vaselli, O., Tassi, F., Grandia, F., Vilanova, E., Mazadiego, L., García-Martínez, M. J., Llamas, J., & Chacón, E. (2011). *Caracterización geoquímica de la línea base de flujo de CO2 en la planta de almacenamiento geológico de Hontomín (Burgos, España)*.

Elío, J., Ortega, M. F., Chacón, E., Mazadiego, L. F., & Grandia, F. (2012). Sampling strategies using the "accumulation chamber" for monitoring geological storage of CO2. *International Journal of Greenhouse Gas Control*, *9*, 303-311. https://doi.org/10.1016/j.ijggc.2012.04.006

Elio Medina, J. de. (2013). *Estrategias de monitorización de CO2 y otros gases en los estudios de análogos naturales* [Phd, E.T.S.I. Minas (UPM)]. https://oa.upm.es/22541/

Epron, D., Farque, L., Lucot, É., & Badot, P.-M. (1999). Soil CO2 efflux in a beech forest: Dependence on soil temperature and soil water content. *Annals of Forest Science*, *56*(3), 221-226. https://doi.org/10.1051/forest:19990304

European Commission. (2024). *Renewable energy targets*. https://energy.ec.europa.eu/topics/renewable-energy/renewable-energy-directive-targets-and-rules/renewable-energy-targets_en

Fang, C., & Moncrieff, J. B. (2001). The dependence of soil CO2 efflux on temperature. *Soil Biology and Biochemistry*, *33*(2), 155-165. https://doi.org/10.1016/S0038-0717(00)00125-5

FAO, 2022. (s. f.). Food and agriculture data. Recuperado 30 de enero de 2025, de https://www.fao.org/faostat/en/#data

Förster, A., Norden, B., Zinck-Jørgensen, K., Frykman, P., Kulenkampff, J., Spangenberg, E., Erzinger, J., Zimmer, M., Kopp, J., Borm, G., Juhlin, C., Cosma, C.-G., & Hurter, S. (2006). Baseline characterization of the CO2SINK geological storage site at Ketzin, Germany. *Environmental Geosciences*, *13*(3), 145-161. https://doi.org/10.1306/eg.02080605016

Gabrielli, P., Poluzzi, A., Kramer, G. J., Spiers, C., Mazzotti, M., & Gazzani, M. (2020). Seasonal energy storage for zero-emissions multi-energy systems via underground hydrogen storage. *Renewable and Sustainable Energy Reviews*, *121*, 109629. https://doi.org/10.1016/j.rser.2019.109629

Gal, F., Pokryszka, Z., Labat, N., Michel, K., Lafortune, S., & Marblé, A. (2019). Soil-Gas Concentrations and Flux Monitoring at the Lacq-Rousse CO2-Geological Storage Pilot Site (French Pyrenean Foreland): From Pre-Injection to Post-Injection. *Applied Sciences*, *9*(4), Article 4. https://doi.org/10.3390/app9040645

Hassan, Q., Algburi, S., Sameen, A. Z., Jaszczur, M., & Salman, H. M. (2023). Hydrogen as an energy carrier: Properties, storage methods, challenges, and future implications. *Environment Systems and Decisions*. https://doi.org/10.1007/s10669-023-09932-z

Hassanpouryouzband, A., Joonaki, E., Edlmann, K., & Haszeldine, R. S. (2021). Offshore Geological Storage of Hydrogen: Is This Our Best Option to Achieve Net-Zero? *ACS Energy Letters*, *6*(6), 2181-2186. https://doi.org/10.1021/acsenergylett.1c00845

Heinemann, N., Alcalde, J., Miocic, J. M., Hangx, S. J. T., Kallmeyer, J., Ostertag-Henning, C., Hassanpouryouzband, A., Thaysen, E. M., Strobel, G. J., Schmidt-Hattenberger, C., Edlmann, K., Wilkinson, M., Bentham, M., Stuart Haszeldine, R., Carbonell, R., & Rudloff, A. (2021a). Enabling large-scale hydrogen storage in porous media – the scientific challenges. *Energy & Environmental Science*, *14*(2), 853-864. https://doi.org/10.1039/D0EE03536J

Heinemann, N., Alcalde, J., Miocic, J. M., Hangx, S. J. T., Kallmeyer, J., Ostertag-Henning, C., Hassanpouryouzband, A., Thaysen, E. M., Strobel, G. J., Schmidt-Hattenberger, C., Edlmann, K., Wilkinson, M., Bentham, M., Stuart Haszeldine, R., Carbonell, R., & Rudloff, A. (2021b). Enabling large-scale hydrogen storage in porous media – the scientific challenges. *Energy & Environmental Science*, *14*(2), 853-864. https://doi.org/10.1039/D0EE03536J

Heinemann, N., Booth, M. G., Haszeldine, R. S., Wilkinson, M., Scafidi, J., & Edlmann, K. (2018). Hydrogen storage in porous geological formations – onshore play opportunities in the midland valley (Scotland, UK). *International Journal of Hydrogen Energy*, *43*(45), 20861-20874. https://doi.org/10.1016/j.ijhydene.2018.09.149

Jongen, M., Pereira, J. S., Aires, L. M. I., & Pio, C. A. (2011). The effects of drought and timing of precipitation on the inter-annual variation in ecosystem-atmosphere

exchange in a Mediterranean grassland. *Agricultural and Forest Meteorology*, *151*(5), 595-606. https://doi.org/10.1016/j.agrformet.2011.01.008

Jul, M. del C. C., Naharro, J. R., & Villar, L. P. del. (2016). La monitorización del CO2 difuso superficial para evaluar la seguridad del almacenamiento de CO2. *Anales de la Real Academia de Doctores de España*, *1*(2), Article 2. https://www.publicacionesrade.es/index.php/arade/article/view/27

Junta de Andalucia. (2023, octubre 9). Aforo de producción de olivar en Andalucía. Campaña 2023-2024 [Aforo de producción de olivar en Andalucía. Campaña 2023-2024]. *RAIF*. https://www.juntadeandalucia.es/agriculturapescaaguaydesarrollorural/raif/aforo-de-produccion-de-olivar-en-andalucia-campana-2023-2024/

Kalam, S., Olayiwola, T., Al-Rubaii, M. M., Amaechi, B. I., Jamal, M. S., & Awotunde, A. A. (2021). Carbon dioxide sequestration in underground formations: Review of experimental, modeling, and field studies. *Journal of Petroleum Exploration and Production*, *11*(1), 303-325. https://doi.org/10.1007/s13202-020-01028-7

Klusman, R. W. (2011). Comparison of surface and near-surface geochemical methods for detection of gas microseepage from carbon dioxide sequestration. *International Journal of Greenhouse Gas Control*, *5*(6), 1369-1392. https://doi.org/10.1016/j.ijggc.2011.07.014

Kooch, Y., Kartalaei, Z. M., Haghverdi, K., & Praeg, N. (2023). Soil function indicators are influenced by land use of different ages: A case study in a semi-arid region. *Science of The Total Environment*, *861*, 160570. https://doi.org/10.1016/j.scitotenv.2022.160570

Kuzyakov, Y. (2006). Sources of CO2 efflux from soil and review of partitioning methods. *Soil Biology and Biochemistry*, *38*(3), 425-448. https://doi.org/10.1016/j.soilbio.2005.08.020

Laier, T., & Øbro, H. (2009). Environmental and safety monitoring of the natural gas underground storage at Stenlille, Denmark. *Geological Society, London, Special Publications*, *313*(1), 81-92. https://doi.org/10.1144/SP313.6

Lardo, E., Palese, A. M., Nuzzo, V., Xiloyannis, C., & Celano, G. (2015a). Variability of total soil respiration in a Mediterranean vineyard. *Soil Research*, *53*(5), 531-541. https://doi.org/10.1071/SR14288

Lardo, E., Palese, A. M., Nuzzo, V., Xiloyannis, C., & Celano, G. (2015b). Variability of total soil respiration in a Mediterranean vineyard. *Soil Research*, *53*(5), 531-541. https://doi.org/10.1071/SR14288

Lei, J., Guo, X., Zeng, Y., Zhou, J., Gao, Q., & Yang, Y. (2021). Temporal changes in global soil respiration since 1987. *Nature Communications*, *12*(1), 403. https://doi.org/10.1038/s41467-020-20616-z

Ma, J., Li, Q., Kempka, T., & Kühn, M. (2019). Hydromechanical Response and Impact of Gas Mixing Behavior in Subsurface CH4 Storage with CO2-Based Cushion Gas. *Energy & Fuels*, *33*(7), 6527-6541. https://doi.org/10.1021/acs.energyfuels.9b00518

Madejón, P., Murillo, J. M., Marañón, T., Cabrera, F., & Soriano, M. A. (2003). Trace element and nutrient accumulation in sunflower plants two years after the Aznalcóllar mine spill. *Science of The Total Environment*, *307*(1), 239-257. https://doi.org/10.1016/S0048-9697(02)00609-5

Maestre, F. T., & Cortina, J. (2003). Small-scale spatial variation in soil CO2 efflux in a Mediterranean semiarid steppe. *Applied Soil Ecology*, *23*(3), 199-209. https://doi.org/10.1016/S0929-1393(03)00050-7

Martínez H, E., Fuentes E, J. P., & Acevedo H, E. (2008). CARBONO ORGÁNICO Y PROPIEDADES DEL SUELO. *Revista de la ciencia del suelo y nutrición vegetal*, *8*(1), 68-96. https://doi.org/10.4067/S0718-27912008000100006

Martin-Gorriz, B., González-Real, M. M., Egea, G., & Baille, A. (2020). Ecosystem respiration of old and young irrigated citrus orchards in a semiarid climate. *Agricultural and Forest Meteorology*, *280*, 107787. https://doi.org/10.1016/j.agrformet.2019.107787

Miocic, J., Heinemann, N., Edlmann, K., Scafidi, J., Molaei, F., & Alcalde, J. (2023). Underground hydrogen storage: A review. *Geological Society, London, Special Publications*, *528*(1), 73-86. https://doi.org/10.1144/SP528-2022-88

Montanaro, G., Doupis, G., Kourgialas, N., Markakis, E., Kavroulakis, N., Psarras, G., Koubouris, G., Dichio, B., & Nuzzo, V. (2023). Management options influence seasonal CO2 soil emissions in Mediterranean olive ecosystems. *European Journal of Agronomy*, *146*, 126815. https://doi.org/10.1016/j.eja.2023.126815

Oliveira, A. M., Beswick, R. R., & Yan, Y. (2021a). A green hydrogen economy for a renewable energy society. *Current Opinion in Chemical Engineering*, *33*, 100701. https://doi.org/10.1016/j.coche.2021.100701

Oliveira, A. M., Beswick, R. R., & Yan, Y. (2021b). A green hydrogen economy for a renewable energy society. *Current Opinion in Chemical Engineering*, *33*, 100701. https://doi.org/10.1016/j.coche.2021.100701

Pablo-Romero, M. del P., Sánchez-Braza, A., & González-Jara, D. (2023). Economic growth and global warming effects on electricity consumption in Spain: A sectoral study. *Environmental Science and Pollution Research*, *30*(15), 43096-43112. https://doi.org/10.1007/s11356-022-22312-5

Panfilov, M., Gravier, G., & Fillacier, S. (2006). *Underground Storage of H2 and H2-CO2-CH4 Mixtures*. cp. https://doi.org/10.3997/2214-4609.201402474

Raich, J. W., & Schlesinger, W. H. (1992). The global carbon dioxide flux in soil respiration and its relationship to vegetation and climate. *Tellus B*, *44*(2), 81-99. https://doi.org/10.1034/j.1600-0889.1992.t01-1-00001.x

Raich, J. W., & Tufekciogul, A. (2000). Vegetation and soil respiration: Correlations and controls. *Biogeochemistry*, *48*(1), 71-90. https://doi.org/10.1023/A:1006112000616

Rayment, M. B., & Jarvis, P. G. (2000). Temporal and spatial variation of soil CO2 efflux in a Canadian boreal forest. *Soil Biology and Biochemistry*, *32*(1), 35-45. https://doi.org/10.1016/S0038-0717(99)00110-8

Romanak, K. D., Bennett, P. C., Yang, C., & Hovorka, S. D. (2012). Process-based approach to CO2 leakage detection by vadose zone gas monitoring at geologic CO2 storage sites. *Geophysical Research Letters*, *39*(15). https://doi.org/10.1029/2012GL052426

Rosen, M. A., & Koohi-Fayegh, S. (2016). The prospects for hydrogen as an energy carrier: An overview of hydrogen energy and hydrogen energy systems. *Energy, Ecology and Environment*, *1*(1), 10-29. https://doi.org/10.1007/s40974-016-0005-z

Rutgers, M., Wouterse, M., Drost, S. M., Breure, A. M., Mulder, C., Stone, D., Creamer, R. E., Winding, A., & Bloem, J. (2016). Monitoring soil bacteria with community-level physiological profiles using Biolog^{TM} ECO-plates in the Netherlands and Europe. *Applied Soil Ecology*, *97*, 23-35. https://doi.org/10.1016/j.apsoil.2015.06.007

Salinas Alcantara, L. (2018). *Emisión de CO2 en suelos de pastizales y bosques*. http://ri.uaemex.mx/handle/20.500.11799/98956

Schlesinger, W. H., & Andrews, J. A. (2000). Soil respiration and the global carbon cycle. *Biogeochemistry*, *48*(1), 7-20. https://doi.org/10.1023/A:1006247623877

Shiva Kumar, S., & Lim, H. (2022). An overview of water electrolysis technologies for green hydrogen production. *Energy Reports*, *8*, 13793-13813. https://doi.org/10.1016/j.egyr.2022.10.127

Tan, S., Ni, X., Yue, K., Liao, S., & Wu, F. (2021). Increased precipitation differentially changed soil CO2 efflux in arid and humid areas. *Geoderma*, *388*, 114946. https://doi.org/10.1016/j.geoderma.2021.114946

Tarkowski, R. (2019). Underground hydrogen storage: Characteristics and prospects. *Renewable and Sustainable Energy Reviews*, *105*, 86-94. https://doi.org/10.1016/j.rser.2019.01.051

Thiyagarajan, S. R., Emadi, H., Hussain, A., Patange, P., & Watson, M. (2022). A comprehensive review of the mechanisms and efficiency of underground hydrogen storage. *Journal of Energy Storage*, *51*, 104490. https://doi.org/10.1016/j.est.2022.104490

Turrini, A., Caruso, G., Avio, L., Gennai, C., Palla, M., Agnolucci, M., Tomei, P. E., Giovannetti, M., & Gucci, R. (2017). Protective green cover enhances soil respiration and native mycorrhizal potential compared with soil tillage in a high-density olive orchard in a long term study. *Applied Soil Ecology*, *116*, 70-78. https://doi.org/10.1016/j.apsoil.2017.04.001

UN. (2025). *Goal 7 | January 2025: Affordable and Clean Energy | Naciones Unidas*. United Nations; United Nations. https://www.un.org/es/node/225820

Wang, Y., Luo, G., Li, C., Ye, H., Shi, H., Fan, B., Zhang, W., Zhang, C., Xie, M., & Zhang, Y. (2023). Effects of land clearing for agriculture on soil organic carbon stocks in drylands: A meta-analysis. *Global Change Biology*, *29*(2), 547-562. https://doi.org/10.1111/gcb.16481

Zeng, L., Sarmadivaleh, M., Saeedi, A., Chen, Y., Zhong, Z., & Xie, Q. (2023). Storage integrity during underground hydrogen storage in depleted gas reservoirs. *Earth-Science Reviews*, *247*, 104625. https://doi.org/10.1016/j.earscirev.2023.104625

Acknowledgments

Lo primero de todo, me gustaría dar las gracias a todos los miembros de Ayterra: Pepe, Juan, Malorid y Mª José, por enseñarme lo que significa formar parte de un equipo, por hacerme las mañanas de trabajo mucho más llevaderas y por transmitirme su pasión e interés por el cuidado del medioambiente y de las personas.

Mención especial a mi padre, quien me abrió las puertas que me condujeron a formar parte del proyecto UNDERGY y cuyo esfuerzo y dedicación han sido fundamentales para que todo saliera como debía.

A Javi Elio y Luis Felipe Mazadiego, por las interminables campañas a través de mares de olivares, las tostadas de pringá por la mañana, las comidas en Choza la Manuela y las historias de vida compartidas. En especial a Javi, por aceptar tutorizarme y por su apoyo incondicional hasta el final.

A mis compañeros biólogos, Alba, Mario y Alberto, por su paciencia y cariño para ayudarme con el tratamiento estadístico de los datos.

A mis amigas, Salud y Esperanza—que bien podrían ser el lema de una agencia de seguros—por inspirarme y darme luz durante todo el proceso.

A Julia, por haber superado su MIR hace poco y porque se merece mucho ser feliz.

A mi madre, a mi hermano y a Daga, por estar siempre ahí.

También quiero agradecer a la UPM por confiarme los costosos equipos de medición durante todo el proyecto.

Y, por último, pero no menos importante, a mí mismo, por no rendirme a pesar de las adversidades, por disfrutar como un niño en el trabajo de campo y por sentirme un verdadero científico, viviendo con ilusión cada paso de la investigación mientras desentrañaba los resultados para la redacción final de mi TFM.

"Una es mas auténtica, cuanto más se parece a lo que ha soñao de si mismo"

- La agrado.